

Data-driven interdiction with asymmetric cost uncertainty: a distributionally robust optimization approach

Sergey S. Ketkov^{†a}, Oleg A. Prokopyev^a

^a*Department of Business Administration, University of Zurich, Zurich, 8032, Switzerland*

Abstract

We consider a class of stochastic interdiction games between an upper-level decision-maker (referred to as a *leader*) and a lower-level decision-maker (referred to as a *follower*), where uncertainty lies in the follower's objective function coefficients. Specifically, the follower's profits (or costs) in our model comprise a random vector, whose probability distribution is estimated independently by the leader and the follower, based on their own data. To address the distributional uncertainty, we formulate a distributionally robust interdiction (DRI) model, where both decision-makers solve conventional distributionally robust optimization problems based on the Wasserstein metric. For this model, we prove asymptotic consistency and derive a polynomial-size mixed-integer linear programming (MILP) reformulation. Furthermore, in our bilevel optimization context, the leader may face uncertainty due to its incomplete knowledge of the follower's data. In this regard, we propose two distinct approximations of the true DRI model, where the leader has incomplete or no information about the follower's data. The first approach employs a pessimistic approximation, which turns out to be computationally challenging and requires the design of a specialized Benders decomposition algorithm. The second approach leverages a robust optimization approach from the leader's perspective. To address the resulting problem, we propose a scenario-based outer approximation that admits a potentially large single-level MILP reformulation and satisfies asymptotic robustness guarantees. Finally, for a class of randomly generated instances of the packing interdiction problem, we evaluate numerically how the information asymmetry and the decision-makers' risk preferences affect the models' out-of-sample performance.

Keywords: Bilevel optimization; Distributionally robust optimization; Interdiction; Mixed-integer programming; Wasserstein distance

1. Introduction

Interdiction forms a broad class of deterministic and stochastic optimization problems, arising, for example, in the military, law-enforcement and infectious disease control contexts; see, e.g., the surveys in [47, 48] and the references therein. A classical *attacker-defender* interdiction model can be viewed as a zero-sum game between two decision-makers: an upper-level decision-maker, commonly referred to as a *leader* (or an attacker), and a lower-level decision-maker, referred to as a *follower* (or a defender). The leader initiates the game by allocating limited interdiction resources to target components that are crucial to the follower's operations. In response, the follower observes the leader's actions and aims to maximize its own profit within the impacted environment. Notably, the leader is informed about

[†]Corresponding author. Email: sergei.ketkov@business.uzh.ch; phone: +41-78-301-85-21
 Preprint submitted to Elsevier

the follower's objective criterion and, therefore, it chooses attacks that minimize the potential profit gained by the follower; see, e.g., the survey in [48] and the references therein.

In this study, we focus on a class of linear min-max interdiction problems of the form:

$$[\mathbf{DI}]: \quad \min_{\mathbf{x} \in X} \max_{\mathbf{y} \in Y(\mathbf{x})} \mathbf{c}^\top \mathbf{y}, \quad (1.1)$$

where

$$X = \{\mathbf{x} \in \{0, 1\}^m : \mathbf{H}\mathbf{x} \leq \mathbf{h}\} \text{ and } Y(\mathbf{x}) = \{\mathbf{y} \in \mathbb{R}_+^n : \mathbf{F}\mathbf{y} + \mathbf{L}\mathbf{x} \leq \mathbf{f}\} \quad (1.2)$$

are, respectively, the leader's and follower's feasible sets. The leader's decision variables \mathbf{x} are restricted to be *binary*, while the follower's decision variables \mathbf{y} are *continuous*. Furthermore, to guarantee the existence of an optimal solution in $[\mathbf{DI}]$, we make the following standard assumption (see, e.g., [52]):

A1. The feasible sets X and $Y(\mathbf{x})$ for each $\mathbf{x} \in X$ are non-empty and bounded.

The vector $\mathbf{c} \in \mathbb{R}^n$ represents deterministic *profits* (or *costs*) related to the follower's decision \mathbf{y} . In particular, as there are no restrictions on the sign of \mathbf{c} , $[\mathbf{DI}]$ describes a broad class of interdiction problems, including, e.g., the min-cost flow and the multicommodity flow interdiction [38, 46, 47], packing interdiction [24], as well as electric grid security problems [44]. It is well known that $[\mathbf{DI}]$ remains strongly *NP*-hard even when the integrality constraints for \mathbf{x} are relaxed; see, e.g., [28, 31].

The aim of this study is to examine a *stochastic* version of $[\mathbf{DI}]$, where the follower's objective function coefficients are subject to uncertainty. In line with the standard framework of data-driven stochastic optimization [8, 25], we assume that \mathbf{c} is a random vector, whose probability distribution is not known a priori and can only be observed through a finite training data set. Specifically, in our bilevel optimization context, it is supposed that both the leader and the follower use their own data sets to estimate the distribution of \mathbf{c} .

To address the distributional uncertainty, we formulate a distributionally robust interdiction (DRI) model, where both decision-makers aim to hedge against the worst-case distributions and realizations of \mathbf{c} . This model assumes that the leader has complete knowledge of the structure of the follower's problem, including access to the follower's data. However, in many real-world settings, key parameters of the follower's problem are not accessible to the leader; see, e.g., [4, 15] and the survey in [5]. For example, in our setting, the follower may deliberately withhold its private data due to conflicting objectives between the two decision-makers. To address this limitation, we develop two alternative DRI models in which the leader has only limited knowledge of the follower's data and needs to estimate both the profit distribution and the true follower's policy.

1.1. Related literature

Uncertainty in interdiction models may arise due to various different factors. For instance, interdiction actions may fail with a certain probability, or key problem parameters, such as arc capacities or arc costs in network interdiction models, could be subject to uncertainty; see, e.g., the surveys in [5, 21, 48] and the references therein. Furthermore, as argued in [5], the sources of uncertainty in bilevel optimization are more complex than those in standard single-level problems. That is, not only

the problem’s parameters may be uncertain but also decisions of one of the decision-makers may only be observed partially by the other decision-maker.

In this literature review, we categorize the most relevant studies according to their approach to uncertainty, with the focus on *robust optimization*, *stochastic programming*, and *distributionally robust optimization* models. In particular, we discuss whether the leader’s and the follower’s decisions are made *before* or *after* the realization of uncertainty and, where appropriate, review the computational complexity and solution approaches for the resulting optimization models.

Robust interdiction models. In robust optimization, uncertain problem parameters are commonly represented using deterministic *uncertainty sets*, and the decision-maker chooses an optimal solution based on the worst-case possible realization of the uncertain parameters; see, e.g., [6, 7]. While robust optimization problems are extensively studied in the context of single-level optimization problems, relatively few studies consider a robust optimization approach in the context of interdiction or more general bilevel optimization problems; see, e.g., [5] and the references therein.

First, we refer to Beck et al. [4], who consider a min-max knapsack interdiction problem, where both the leader’s and the follower’s decision variables are integer, while the follower does not have full information about its objective function or constraint coefficients. The authors model the uncertainty using budget-constrained uncertainty sets [9] and propose a general branch-and-cut framework for solving the resulting problem. Notably, the leader in [4] has complete information about the follower’s uncertainty set, whereas both decision-makers implement their decisions *here-and-now*, prior to the realization of uncertainty.

Another relevant study is by Buchheim et al. [15], which examines bilevel linear problems with binary decision variables for the leader and continuous decision variables for the follower. Specifically, the only difference between [DI] and the model in [15] is that the latter allows different objective function coefficients for the leader and the follower. Buchheim et al. [15] assume that the leader has incomplete information about the follower’s objective function coefficients and estimates them using either interval or discrete uncertainty sets. As a result, the leader in [15] makes a here-and-now decision, while the follower makes a *wait-and-see* decision, affected by the realization of uncertainty. Buchheim et al. [15] show that, under interval uncertainty, the resulting robust bilevel problem is Σ_p^2 -hard. In other words, this problem is located at the second level of the polynomial hierarchy and there is no way of formulating it as a single-level linear mixed-integer programming (MILP) problem of polynomial size, unless the polynomial hierarchy collapses; see, e.g., [31]. On a positive note, it is established in [15] that, under discrete uncertainty, the problem is at most one level harder than the follower’s problem.

Then, several recent studies consider robust formulations in the context of network interdiction problems. For example, Azizi and Seifi [2] consider the shortest path network interdiction problem, where the follower is uncertain about the additional costs imposed for traversing interdicted arcs. The authors consider here-and-now decision-makers, represent the uncertain parameters using a budget-constrained uncertainty set, and solve the resulting robust problem by using its single-level dual reformulation. In contrast, Chauhan et al. [18] study a robust maximum flow interdiction problem with a wait-and-see follower, considering uncertain arc capacities and interdiction resources. The problem is

approximated by a single-level MILP reformulation and then addressed using three heuristics designed for this problem and its underlying network structure. Finally, we refer to the studies in [13, 14] for multi-stage interdiction models with incomplete information, in which the leader refines its information about the follower’s costs and the structure of the follower’s problem by observing the follower’s actions.

Stochastic interdiction models. In stochastic optimization, uncertain problem parameters are typically assumed to follow a fixed and known probability distribution, and the goal is to optimize a risk measure such as the expected value or the conditional value-at-risk (CVaR) based on this distribution; see, e.g., [10, 42, 45]. Most of the existing literature considers stochastic interdiction problems involving a *risk-neutral* leader, whose objective is to minimize the follower’s expected utility; see, e.g., [21, 30, 39] and the survey in [48]. In contrast, we focus on *risk-averse* stochastic interdiction models, where the decision-makers account for the risks associated with the realization of uncertain parameters and aim to mitigate the impact of extremely large losses.

Of particular relevance to our model is the study by Lei et al. [37], which explores a stochastic maximum flow interdiction model with here-and-now decision-makers. In their framework, the arc capacities and the effects of interdiction actions follow a discrete probability distribution defined by a finite set of *scenarios* and associated probabilities. Furthermore, the follower can introduce additional arc capacities for mitigating flow losses, after knowing the leader’s interdiction plan but before realizing the uncertainty. The leader and the follower in [37] seek to minimize and maximize, respectively, the right- and the left-tail CVaR; see, e.g., [42]. That is, since the decision-makers have conflicting objective functions, the pessimism of one decision-maker naturally translates to an optimistic viewpoint for the other. Based on the strong duality, Lei et al. [37] propose various MILP reformulations of the resulting problem, depending on the decision-makers’ risk preferences.

Next, Song and Shen [49] and Pay et al. [40] consider a stochastic shortest path interdiction problem with uncertain travel times and interdiction effects. Both models assume a known discrete distribution of the uncertain problem parameters and focus on the case of a here-and-now leader and a wait-and-see follower. Song and Shen [49] introduce a chance constraint on the length of the follower’s shortest path and address the resulting problem using a branch-and-cut algorithm. On the other hand, Pay et al. [40] assume ambiguous risk-preferences from the leader’s perspective. In this regard, the authors provide several approaches to optimization over a class of utility functions.

Finally, Atamtürk et al. [1] consider mean-risk maximum flow interdiction problem with uncertain arc capacities. In contrast to the scenario-based approach, the model presented in [1] assumes that the uncertain problem parameters follow a nearly normal distribution, characterized by a known mean and a known covariance matrix. Then, the problem of minimizing the maximum flow-at-risk over a discrete set of actions is reduced to a sequence of discrete quadratic optimization problems.

Distributionally robust interdiction models. Distributionally robust optimization (DRO) models assume that the distribution of uncertain problem parameters is unknown and belongs to an *ambiguity set* of plausible distributions; see, e.g., [22, 25, 51] and the review in [41]. Then, similar to robust optimization, the decision-maker selects an optimal solution based on the worst-case distribution of the uncertain parameters. Overall, one-stage DRO models can often be reformulated as tractable convex optimization problems and provide, on average, a better out-of-sample performance

compared to stochastic programming models constrained to a single candidate distribution [25, 51].

To the best of our knowledge, there are only a few studies that examine a DRO approach in the context of interdiction problems. Notably, Sadana and Delage [43], analyze the value of randomization for a class of distributionally robust risk-averse maximum flow interdiction problems. Specifically, it is assumed that the arc capacities are subject to distributional uncertainty and the ambiguity set is comprised of *discrete* distributions concentrated around a fixed reference distribution. The leader in [43] randomizes over the feasible interdiction plans in order to minimize the worst-case CVaR of the maximum flow with respect to both the unknown distribution of the capacities and its own randomized strategy. Meanwhile, the follower makes a wait-and-see decision by solving a maximum flow problem with given arc capacities. Sadana and Delage [43] reformulate the leader’s DRO problem as a bilinear optimization problem and solve it using a specialized spatial branch-and-bound algorithm.

In conclusion, we refer to Kang and Bansal [32], who investigate multistage *risk-neutral* stochastic mixed-integer programs. In the context of network interdiction, the authors account for uncertainty in arc capacities and interdiction effects, considering a leader who may be either ambiguity-averse or ambiguity-receptive. In these two variations of the problem, the leader focuses, respectively, on the worst-case and the best-case expected losses incurred by the follower. Similar to the work of Sadana et al. [43], both formulations involve a wait-and-see follower but allow for discrepancy-based ambiguity sets based on the Wasserstein metric. To solve both problem versions, Kang and Bansal [32] propose several exact solution methods that leverage decomposition and reformulation techniques.

1.2. Our approach and contributions

In this paper, we analyze a *data-driven distributionally robust interdiction* (DRI) problem associated with **[DI]**, where the profit vector \mathbf{c} is subject to distributional uncertainty. That is, the leader and the follower in our model are given two distinct training data sets drawn from the unknown *true distribution* of \mathbf{c} . As outlined earlier, the inherent conflict between the decision-makers suggests that the leader may also face uncertainty in the follower’s private data and, consequently, in the follower’s optimal decision. Accordingly, we develop three optimization models, reflecting different levels of the leader’s knowledge about the follower’s data.

First, we introduce a *basic DRI model*, where the leader has complete knowledge of the follower’s data and, furthermore, the follower’s data set is included in the leader’s. The latter assumption follows naturally, as both data sets are used to estimate the *same* probability distribution. That is, the only source of uncertainty in our basic model is associated with the distribution of \mathbf{c} .

To address the distributional uncertainty, we employ data-driven ambiguity sets based on the Wasserstein distance from the empirical distribution of the data; see, e.g., [25, 26]. More specifically, similar to Lei et al. [37], both decision-makers in our model solve conventional one-stage Wasserstein DRO problems based on the conditional value-at-risk (CVaR) and act *here-and-now*, prior to the realization of uncertainty. Our choice of the ambiguity sets is justified by the fact that one-stage Wasserstein DRO models effectively balance tractability and statistical guarantees, leading to their broad applications in machine learning, portfolio optimization and network routing problems; see, e.g., [11, 36, 50]. Finally, following the major part of the bilevel optimization literature, we consider

an *optimistic* formulation of the resulting bilevel problem. That is, if the follower has multiple optimal solutions, then the most favorable to the leader is preferred; see, e.g., the surveys in [20, 35], and the references therein.

For the models with incomplete knowledge of the follower’s data, we first introduce a hypothetical *true basic DRI model*, in which the leader has full knowledge of the follower’s data set, but this set is not a subset of the leader’s. We then propose two approximations of the true basic model. In the *pessimistic approximation*, the leader disregards any available information about the follower’s data and optimizes its own objective function with respect to the worst-case feasible follower’s policy. On the other hand, in the *semi-pessimistic approximation*, we adopt a robust optimization approach from the leader’s perspective and assume that the follower’s data set is subject to component-wise *interval uncertainty*. That is, similar to the one-stage DRO model with data uncertainty in [34], the leader optimizes its objective function assuming the worst-case possible realization of the follower’s data within the uncertainty set.

Our main theoretical contributions can be summarized as follows:

- First, provided that the Wasserstein ambiguity sets for both decision-makers are defined in terms of ℓ_1 - or ℓ_∞ -norm, we establish the computational complexity for all proposed optimization models. That is, while the basic DRI model is *NP*-hard, both pessimistic and semi-pessimistic approximations turn out to be Σ_2^P -hard. To prove our complexity results, we use reductions from the dominating set interdiction and the robust bilevel interdiction problem with interval uncertainty that are known to be Σ_2^P -hard [15, 27].
- In line with the one-stage DRO models in [25, 26], we demonstrate that, under mild assumptions, the basic DRI model is *asymptotically consistent*. That is, when the leader and the follower acquire more data, their optimal solutions and the respective optimal objective function values converge, in a sense, to those of the underlying stochastic programming problem. To the best of our knowledge, this is the first result in the literature that establishes convergence of DRO models in a bilevel problem setting.
- The basic DRI model is reformulated and solved as a single-level MILP problem of polynomial size. This reformulation builds on linear programming reformulations of the worst-case CVaR problems for both decision-makers [25] and a strong duality-based reformulation of the follower’s problem; see, e.g., [52].
- To address the pessimistic approximation, we design a Benders decomposition algorithm tailored to two special cases of the problem, where the leader is either *risk-neutral* or *ambiguity-free*. The algorithm for each case is based on the standard decomposition techniques for bilevel optimization [29, 53] and leverages a disjoint bilinear structure of the inner optimization problem.
- To address the semi-pessimistic approximation, we propose a scenario-based discretization of the leader’s uncertainty set. This approach, as indicated in [15], reduces the computational complexity and enables a unified MILP reformulation of the problem. To justify our approach, we show that the discretized semi-pessimistic approximation is almost surely *robust* with respect to the follower’s data in an asymptotic sense, i.e., when the number of scenarios tends to infinity.

Despite the fact that some standard no-good cuts can be applied to general bilevel interdiction problems with a non-convex lower level [12], Σ_2^P -hard problems remain notoriously difficult, even for medium-sized problem instances. For this reason, the focus of our study is on solution techniques tailored to the structure of the proposed approximations.

		Our paper	Lei et al. [37]	Sadana & Delage [43]
Follower	here-and-now	✓	✓	✗
	wait-and-see	✗	✗	✓
Follower's decision variables	continuous	✓	✓	✓
	integer	✗	✗	✗/✓
Uncertainty	scenario-based	✗	✓	✓
	data-driven	✓	✗	✗
	objective function	✓	✓	✓
	constraints	✗	✓	✓
Risk-aversion	leader	✓	✓	✓
	follower	✓	✓	✗
Ambiguity-aversion	leader	✓	✗	✓
	follower	✓	✗	✗
Information asymmetry		✓	✗	✗

Table 1: Comparison of our model with the related models in [37] and [43]. Symbol ✗/✓ indicates that the model in [43] can only be applied to the follower's problem with a unimodular constraint matrix.

Contributions to the related literature. In view of the discussion above, we compare our DRI model with the most related studies in Lei et al. [37] and Sadana and Delage [43]; see Table 1. Our contributions can be summarized as follows:

- To the best of our knowledge, our model is the first in the interdiction literature to incorporate data-driven distributional uncertainty and information asymmetry with respect to the data.
- Unlike the studies in [37, 43], we incorporate risk aversion and ambiguity aversion for both decision-makers, thereby adopting the standard conventions of one-stage DRO models.
- Beyond the standard distributional uncertainty arising from the decision-makers' incomplete knowledge of the true data-generating distribution, our model also examines uncertainty in the follower's decision caused by the leader's limited knowledge of the follower's data.

Given these advantages, our model also has two major limitations. First, unlike existing interdiction models with a wait-and-see follower [40, 43, 49], our approach cannot address interdiction problems with a unimodular structure at the lower level [29, 54]. Instead, we focus on a more specific class of interdiction problems, such as the min-cost flow or the multicommodity flow interdiction problems [38], as well as the packing interdiction problem [24], where the follower's continuous decisions have a natural interpretation; see row 2 of Table 1. Secondly, we account for uncertainty in the follower's objective function coefficients but not in the follower's *constraints*; see row 3 of Table 1. In this regard, we observe that distributionally robust chance-constrained problems with a Wasserstein ambiguity set do not allow for a linear programming (LP) reformulation [19] and, therefore, make even the basic DRI model com-

putationally challenging. On a positive note, with a slight modification, our model can also address uncertainty in the interdiction effects, since this uncertainty appears in the follower's objective function.

The remainder of the paper is organized as follows. First, in Section 2, we introduce a full information stochastic programming model and our modeling assumptions. Next, in Sections 3–5, we analyze the basic, pessimistic and semi-pessimistic DRI models, respectively, along with their theoretical properties and corresponding solution methods. In Section 6, we perform a numerical analysis of the proposed DRI models using a set of randomly generated instances of the packing interdiction problem. Finally, Section 7 provides conclusions and outlines possible directions for future research.

Notation. All vectors and matrices are denoted by bold letters. A vector of all ones is represented as $\mathbf{1}$ and a diagonal matrix with vector \mathbf{x} on the diagonal is referred to as $\text{diag}(\mathbf{x})$. Also, $\dim(\mathbf{x})$ refers to the dimension of \mathbf{x} . We use \mathbb{R}_+ to denote the set of nonnegative real numbers and \mathbb{Z}_+ (\mathbb{N}) to denote the set of nonnegative (positive) integers. Additionally, subscripts “ l ” and “ f ” refer to parameter's of the leader's and the follower's problems, respectively. For $a \in \mathbb{R}$, we use a standard notation $a^+ = \max\{a; 0\}$ and $a^- = \min\{a; 0\}$. For a given support set $S \subseteq \mathbb{R}^n$, let $\mathcal{Q}_0(S)$ denote the space of all probability distributions defined on S . Finally, the k -fold product of a distribution $\mathbb{Q} \in \mathcal{Q}_0(S)$ is denoted by \mathbb{Q}^k , which represents a distribution on the Cartesian product space S^k .

2. Model setup and assumptions

Full information model. Let $\mathbb{Q}^* \in \mathcal{Q}_0(S)$ represent a true (nominal) distribution of the profit vector \mathbf{c} , supported on $S \subseteq \mathbb{R}^n$. Ideally, with complete knowledge of \mathbb{Q}^* , our goal is to solve the following stochastic programming formulation of [DI]:

$$[\text{SI}]: \quad z^* := \min_{\mathbf{x}, \mathbf{y}} \rho_l(\mathbf{y}, \mathbb{Q}^*) \quad (2.1a)$$

$$\text{s.t. } \mathbf{x} \in X \quad (2.1b)$$

$$\mathbf{y} \in \operatorname{argmax}_{\tilde{\mathbf{y}} \in Y(\mathbf{x})} \rho_f(\tilde{\mathbf{y}}, \mathbb{Q}^*), \quad (2.1c)$$

where $\rho_l(\mathbf{y}, \mathbb{Q}^*)$ and $\rho_f(\mathbf{y}, \mathbb{Q}^*)$ denote the leader's and the follower's risk functions, and the minimization with respect to \mathbf{y} in (2.1a) implies an optimistic version of the bilevel problem; recall our discussion in Section 1.2.

Following the model of Lei et al. [37], we define $\rho_l(\mathbf{y}, \mathbb{Q}^*)$ and $\rho_f(\mathbf{y}, \mathbb{Q}^*)$ using the right-tail and the left-tail conditional values-at-risk (CVaRs), respectively. That is, given confidence levels $\alpha_l \in (0, 1)$ and $\alpha_f \in (0, 1)$, we have:

$$\rho_l(\mathbf{y}, \mathbb{Q}^*) := \min_{t_l \in \mathbb{R}} \left\{ t_l + \frac{1}{1 - \alpha_l} \mathbb{E}_{\mathbb{Q}^*} \{ (\mathbf{c}^\top \mathbf{y} - t_l)^+ \} \right\} \quad \text{and} \quad (2.2a)$$

$$\rho_f(\mathbf{y}, \mathbb{Q}^*) := \max_{t_f \in \mathbb{R}} \left\{ t_f + \frac{1}{1 - \alpha_f} \mathbb{E}_{\mathbb{Q}^*} \{ (\mathbf{c}^\top \mathbf{y} - t_f)^- \} \right\}, \quad (2.2b)$$

where an equivalent representation of CVaR due to [42] is employed. In this context, the right-tail CVaR (2.2a) and the left-tail CVaR (2.2b) measure the expected value of extremely high losses for the leader (i.e., upper-tail risk) and extremely low profits for the follower (i.e., lower-tail risk), respectively.

Notably, both risk measures reduce to the expected value of $\mathbf{c}^\top \mathbf{y}$ under \mathbb{Q}^* in the limiting cases of $\alpha_l = 0$ and $\alpha_f = 0$. Consequently, by choosing appropriate confidence levels, α_l and α_f , the decision-makers can adjust their level of risk-aversion.

Distributional uncertainty. To address the distributional uncertainty regarding \mathbb{Q}^* , we make the following assumptions about the partial distributional information available to the decision-makers:

A2. The *support* of \mathbb{Q}^* is known and given by a non-empty compact polyhedral set

$$S = \left\{ \mathbf{c} \in \mathbb{R}^n : \mathbf{B}\mathbf{c} \leq \mathbf{b} \right\}. \quad (2.3)$$

A3. The leader and the follower have access to two independent and identically distributed (i.i.d.) training data sets, generated according to \mathbb{Q}^* ,

$$\hat{\mathbf{C}}_l = \left\{ \hat{\mathbf{c}}_l^{(k)} \in S, k \in K_l := \{1, \dots, k_l\} \right\} \text{ and } \hat{\mathbf{C}}_f = \left\{ \hat{\mathbf{c}}_f^{(k)} \in S, k \in K_f := \{1, \dots, k_f\} \right\}. \quad (2.4)$$

Furthermore, $\hat{\mathbf{C}}_f \subseteq \hat{\mathbf{C}}_l$ or, equivalently, $k_f \leq k_l$ and $\hat{\mathbf{c}}_f^{(k)} = \hat{\mathbf{c}}_l^{(k)}$ for each $k \in K_f$.

Both Assumptions **A2** and **A3** align with the standard one-stage DRO models in [22, 25, 51] and offer a natural, myopic extension to our bilevel interdiction problem setting. Notably, Assumption **A2** also requires compactness of the support set S . This assumption simplifies our convergence analysis and naturally fits interdiction problems, where uncertain problem parameters usually come from a finite set of scenarios [37, 43] or satisfy specified interval constraints [13, 15]. Finally, the second part of Assumption **A3** indicates that the leader needs full information about the follower's feasible set, including the follower's data; recall our discussion of the basic DRI model in Section 1.2.

Next, following conventional Wasserstein DRO models in [25, 26], we define each decision-maker's ambiguity set as a type-1 Wasserstein ball, centered at their empirical data distribution. Specifically, for $i \in \{l, f\}$, the ambiguity set is given by:

$$\mathcal{Q}_i := \left\{ \mathbb{Q} \in \mathcal{Q}_0(S) : W^p(\hat{\mathbb{Q}}_i, \mathbb{Q}) \leq \varepsilon_i \right\}, \quad (2.5)$$

where

$$\hat{\mathbb{Q}}_i(\hat{\mathbf{C}}_i) := \frac{1}{k_i} \sum_{k \in K_i} \delta(\hat{\mathbf{c}}_i^{(k)}), \quad i \in \{l, f\},$$

is the empirical distribution of the observed data, with $\delta : \mathbb{R} \rightarrow \mathbb{R}$ representing the Dirac delta function, and $\varepsilon_i \in \mathbb{R}_+$ is the Wasserstein radius. Furthermore, given that $\Pi(\hat{\mathbb{Q}}_i, \mathbb{Q})$ is the set of all couplings with marginals $\hat{\mathbb{Q}}_i$ and \mathbb{Q} ,

$$W^p(\hat{\mathbb{Q}}_i, \mathbb{Q}) := \inf_{\pi \in \Pi(\hat{\mathbb{Q}}_i, \mathbb{Q})} \int_{S \times S} \|\hat{\mathbf{c}}_i - \mathbf{c}\|_p \pi(d\hat{\mathbf{c}}_i, d\mathbf{c}), \quad i \in \{l, f\},$$

denotes the type-1 Wasserstein distance between $\hat{\mathbb{Q}}_i$ and \mathbb{Q} with respect to the ℓ_p -norm [33].

In the following, we focus on the Wasserstein distance with respect to ℓ_1 - or ℓ_∞ -norm, since computing the worst-case CVaR within such Wasserstein balls is equivalent to solving a finite linear

programming (LP) problem; see Corollary 5.1 in [25]. Finally, the radii ε_i , $i \in \{l, f\}$, are typically selected to ensure that the true distribution \mathbb{Q}^* belongs to the Wasserstein ambiguity sets with high probability; see, e.g., [25, 26]. We discuss our choice of ε_l and ε_f in more detail within Section 6.

To motivate our basic DRI model, as well as the pessimistic and the semi-pessimistic approximations discussed in Section 1.2, we present the following illustrative example.

Model	Optimal leader's decision	Leader's estimated objective	Leader's true objective
Full information	$(0, 0, 1, 1)^\top$	6	6
True basic	$(0, 0, 0, 1)^\top$	7	9
Pessimistic	$(1, 1, 0, 0)^\top$	8	10
Semi-pessimistic	$(0, 0, 0, 1)^\top$	7	9
Augmented basic	$(1, 1, 0, 0)^\top$	8	10

Table 2: Optimal solutions and the respective leader's estimated and true objective function values under optimization models (2.6)–(2.10), respectively, discussed in Example 1.

Example 1. Consider an instance of the packing interdiction problem [24] with uncertain profits given by:

$$\min_{\mathbf{x} \in X} \max_{\mathbf{y} \in Y(\mathbf{x})} \mathbf{c}^\top \mathbf{y},$$

where

$$X = \left\{ \mathbf{x} \in \{0, 1\}^4 : \sum_{i=1}^4 x_i \leq 2 \right\} \quad \text{and} \quad Y(\mathbf{x}) = \left\{ \mathbf{y} \in [0, 1]^4 : \mathbf{y} \leq \mathbf{1} - \mathbf{x}, \sum_{i=1}^4 y_i \leq 1 \right\}$$

are, respectively, the leader's and the follower's feasible sets. Assume that the follower's profit vector \mathbf{c} belongs to a support set

$$S = \left\{ \mathbf{c} \in \mathbb{R}^4 : c_1 \in [0, 10], c_2 \in [1, 11], c_3 \in [6, 12], c_4 \in [7, 13] \right\},$$

with the true distribution \mathbb{Q}^* being a *discrete uniform distribution* on S .

Given that both decision-makers are risk-neutral, i.e., $\alpha_l = 0$ and $\alpha_f = 0$, the full information model [SI] reads as:

$$z^* = \min_{\mathbf{x} \in X} \max_{\mathbf{y} \in Y(\mathbf{x})} \bar{\mathbf{c}}^*{}^\top \mathbf{y}, \tag{2.6}$$

where $\bar{\mathbf{c}}^* = (5, 6, 9, 10)^\top$ is a vector of the true expected costs. The optimal solution of (2.6) is given by $\mathbf{x}^* = (0, 0, 1, 1)^\top$, with the true expected profit of the follower $z^* = 6$; see Table 2.

Next, for simplicity, we assume that $\varepsilon_l = \varepsilon_f = 0$, i.e., both the leader and the follower implement a myopic *sample average approximation* based on $k_l = k_f = 5$ samples given by:

$$\hat{\mathbf{C}}_l = \begin{pmatrix} 10 & 11 & 8 & 7 \\ 6 & 7 & 7 & 9 \\ 10 & 10 & 7 & 9 \\ 9 & 11 & 6 & 7 \\ 10 & 11 & 7 & 8 \end{pmatrix} \quad \text{and} \quad \hat{\mathbf{C}}_f = \begin{pmatrix} 3 & 3 & 8 & 13 \\ 1 & 2 & 9 & 10 \\ 3 & 11 & 11 & 13 \\ 10 & 3 & 10 & 12 \\ 4 & 1 & 12 & 7 \end{pmatrix},$$

with average profits

$$\bar{\mathbf{c}}_l := (9, 10, 7, 8)^\top \quad \text{and} \quad \bar{\mathbf{c}}_f := (4, 5, 10, 11)^\top,$$

respectively. Clearly, in this setting, the second part of Assumption **A3** does not hold, i.e., $\hat{\mathbf{C}}_f \not\subseteq \hat{\mathbf{C}}_l$.

Therefore, we first formulate a hypothetical *true basic model* defined as:

$$z_b^* := \min_{\mathbf{x}, \mathbf{y}} \bar{\mathbf{c}}_l^\top \mathbf{y} \quad (2.7a)$$

$$\text{s.t. } \mathbf{x} \in X \quad (2.7b)$$

$$\mathbf{y} \in \operatorname{argmax}_{\tilde{\mathbf{y}} \in Y(\mathbf{x})} \bar{\mathbf{c}}_f^\top \tilde{\mathbf{y}}, \quad (2.7c)$$

where the leader makes no errors in estimating the true follower's policy. To address uncertainty in the follower's data, we consider the following three possible approaches:

(i) The leader may solve a *pessimistic approximation* of (2.7) given by:

$$\hat{z}_p^* = \min_{\mathbf{x} \in X} \max_{\mathbf{y} \in Y(\mathbf{x})} \bar{\mathbf{c}}_l^\top \mathbf{y}. \quad (2.8)$$

The leader in (2.8) disregards any information about the follower's data and minimizes its objective function value assuming the worst-case feasible follower's policy.

(ii) Alternatively, assume that the leader has partial information about the follower's data, e.g., it is aware of the first two components in $\hat{\mathbf{C}}_f$. In this case, the leader may solve a *semi-pessimistic approximation* of (2.7) given by:

$$\hat{z}_{sp}^* := \min_{\mathbf{x} \in X} \max_{\bar{\mathbf{c}}_f \in \bar{S}_l} \min_{\mathbf{y}} \bar{\mathbf{c}}_l^\top \mathbf{y} \quad (2.9a)$$

$$\text{s.t. } \mathbf{y} \in \operatorname{argmax}_{\tilde{\mathbf{y}} \in Y(\mathbf{x})} \bar{\mathbf{c}}_f^\top \tilde{\mathbf{y}}, \quad (2.9b)$$

where

$$\bar{S}_l = \left\{ \bar{\mathbf{c}} \in \mathbb{R}^4 : \bar{c}_1 = 4, \bar{c}_2 = 5, \bar{c}_3 \in [6, 12], \bar{c}_4 \in [7, 13] \right\}.$$

In other words, based on the partial information about $\hat{\mathbf{C}}_f$, the leader in (2.9) may construct the uncertainty set \bar{S}_l for the follower's average profits $\bar{\mathbf{c}}_f$ and account for the worst-case scenario within this set.

(iii) To enforce Assumption **A3**, one may assume that the leader generates the missing samples, e.g., by resampling from its own data set. In our case, since the decision-makers' data sets have the same size, we assume for simplicity that the leader's data set is used *instead* of the follower's data set. In other words, the leader may solve an *augmented basic model* of the form:

$$\hat{z}_{ab}^* := \min_{\mathbf{x}, \mathbf{y}} \bar{\mathbf{c}}_l^\top \mathbf{y} \quad (2.10a)$$

$$\text{s.t. } \mathbf{x} \in X \quad (2.10b)$$

$$\mathbf{y} \in \operatorname{argmax}_{\tilde{\mathbf{y}} \in Y(\mathbf{x})} \bar{\mathbf{c}}_l^\top \tilde{\mathbf{y}}. \quad (2.10c)$$

Within this example, (2.10) coincides with the pessimistic approximation (2.8). However, in general, these are two distinct models, as the objective functions of the leader and the follower may vary.

For each of the outlined models, we provide the leader's optimal solution along with the corresponding estimated and true objective function values in Table 2. For all models except the full information model, the true value is computed under the true follower's policy, as defined in (2.7), and the true distribution \mathbb{Q}^* . \square

We draw several important observations from Example 1. First, both the leader and the follower may experience out-of-sample errors due to inaccuracies in their perception of the profit vector \mathbf{c} . For example, replacing the expected profit vector $\bar{\mathbf{c}}^*$ with the leader's estimate $\bar{\mathbf{c}}_l$ in the true basic model (2.7) increases the follower's true expected profit from 6 to 9. Another important source of error arises from the leader's incorrect estimate of the follower's policy. For instance, the augmented basic model (2.10) and the pessimistic approximation (2.8) further increase the true follower's profit from 9 to 10, which is not the case for the semi-pessimistic approximation (2.9). To provide additional practical insights, we investigate the effect of these errors numerically in Section 6.

Secondly, we observe that the optimal objective function values in (2.7), (2.8) and (2.9) satisfy the following hierarchy:

$$z_b^* \leq \hat{z}_{sp}^* \leq \hat{z}_p^*.$$

Specifically, in Example 1, we have $z_b^* = \hat{z}_{sp}^* = 7$ and $\hat{z}_p^* = 8$. The inequality $\hat{z}_{sp}^* < \hat{z}_p^*$ suggests that, even with partial information about the follower's data, the leader may potentially refine its estimate of the true follower's policy and thereby improve its in-sample performance. Finally, the optimal objective function value of (2.10), \hat{z}_{ab}^* , does not have any specific relationship with z_b^* and, therefore, the augmented basic model (2.10) is only discussed within our numerical study in Section 6.

3. Basic DRI model

3.1. Problem formulation and solution approach

In contrast to the full information model [SI], we assume that the true distribution \mathbb{Q}^* is known to the leader and the follower only partially, as specified by Assumptions **A2** and **A3**. Then, the basic distributionally robust interdiction (DRI) model is formulated as:

$$[\mathbf{DRI}]: \quad \hat{z}_b^* := \min_{\mathbf{x}, \mathbf{y}} \left\{ \max_{\mathbb{Q}_l \in \mathcal{Q}_l} \rho_l(\mathbf{y}, \mathbb{Q}_l) \right\} \quad (3.1a)$$

$$\text{s.t. } \mathbf{x} \in X \quad (3.1b)$$

$$\mathbf{y} \in \operatorname{argmax}_{\tilde{\mathbf{y}} \in Y(\mathbf{x})} \left\{ \min_{\mathbb{Q}_f \in \mathcal{Q}_f} \rho_f(\tilde{\mathbf{y}}, \mathbb{Q}_f) \right\}, \quad (3.1c)$$

where the data-driven ambiguity sets \mathcal{Q}_l and \mathcal{Q}_f are defined by equation (2.5). Additionally, the risk functions $\rho_l(\mathbf{y}, \mathbb{Q}_l)$ and $\rho_f(\mathbf{y}, \mathbb{Q}_f)$ are defined similar to equations (2.2a) and (2.2b), i.e.,

$$\rho_l(\mathbf{y}, \mathbb{Q}_l) := \min_{t_l \in \mathbb{R}} \left\{ t_l + \frac{1}{1 - \alpha_l} \mathbb{E}_{\mathbb{Q}_l} \{ (\mathbf{c}^\top \mathbf{y} - t_l)^+ \} \right\} \quad \text{and} \quad (3.2a)$$

$$\rho_f(\mathbf{y}, \mathbb{Q}_f) := \max_{t_f \in \mathbb{R}} \left\{ t_f + \frac{1}{1 - \alpha_f} \mathbb{E}_{\mathbb{Q}_f} \{ (\mathbf{c}^\top \mathbf{y} - t_f)^- \} \right\}, \quad (3.2b)$$

where $\alpha_l \in (0, 1)$ and $\alpha_f \in (0, 1)$ are the prespecified confidence levels.

Importantly, the compactness of the support set S (Assumption **A2**) ensures the existence of the worst-case distributions in (3.1a) and (3.1c), allowing the supremum (infimum) over the ambiguity sets to be replaced by the maximum (minimum); see Corollary 4.6 in [25]. Moreover, we implicitly assume that the leader in **[DRI]** has full information about the follower's feasible set $Y(\mathbf{x})$ and two global parameters, α_f and ε_f ; possible relaxations of this assumption are briefly discussed in Section 6.5. The following results provide an MILP reformulation of **[DRI]**.

Lemma 1. *Let Assumptions **A1-A3** hold, and the ambiguity sets in (2.5) be defined in terms of p -norm with $p \in \{1, \infty\}$. Then, for any fixed $\mathbf{x} \in X$, the follower's problem*

$$\max_{\mathbf{y} \in Y(\mathbf{x})} \min_{\mathbb{Q}_f \in \mathcal{Q}_f} \rho_f(\mathbf{y}, \mathbb{Q}_f) \quad (3.3)$$

can be equivalently reformulated as a linear programming (LP) problem of the form:

$$\max_{\mathbf{y}, \boldsymbol{\nu}_f, \mathbf{s}_f, \lambda_f, t_f} \left\{ t_f - \frac{1}{1 - \alpha_f} \left(\varepsilon_f \lambda_f + \frac{1}{k_f} \sum_{k \in K_f} s_f^{(k)} \right) \right\} \quad (3.4a)$$

$$\text{s.t. } \mathbf{F}\mathbf{y} \leq \mathbf{f} - \mathbf{L}\mathbf{x} \quad (3.4b)$$

$$\left. \begin{aligned} -\hat{\mathbf{c}}_f^{(k)\top} \mathbf{y} + t_f + \boldsymbol{\Delta}_f^{(k)\top} \boldsymbol{\nu}_f^{(k)} &\leq s_f^{(k)} \\ \|\mathbf{B}^\top \boldsymbol{\nu}_f^{(k)} + \mathbf{y}\|_q &\leq \lambda_f \\ \boldsymbol{\nu}_f^{(k)} &\geq \mathbf{0}, \quad s_f^{(k)} \geq 0 \end{aligned} \right\} \forall k \in K_f \quad (3.4c)$$

$$\mathbf{y} \geq \mathbf{0}, \quad (3.4d)$$

where $\boldsymbol{\Delta}_f^{(k)} = \mathbf{b} - \mathbf{B}\hat{\mathbf{c}}_f^{(k)} \geq \mathbf{0}$ for each $k \in K_f$ and $\frac{1}{p} + \frac{1}{q} = 1$. Furthermore, (3.4) admits the following equivalent dual reformulation:

$$\min_{\bar{\boldsymbol{\mu}}_f, \underline{\boldsymbol{\mu}}_f, \boldsymbol{\beta}_f, \boldsymbol{\gamma}_f} \left\{ (-\mathbf{L}\mathbf{x} + \mathbf{f})^\top \boldsymbol{\beta}_f \right\} \quad (3.5a)$$

$$\text{s.t. } \mathbf{F}^\top \boldsymbol{\beta}_f - \sum_{k \in K_f} \gamma_f^{(k)} \hat{\mathbf{c}}_f^{(k)} + \sum_{k \in K_f} (\bar{\boldsymbol{\mu}}_f^{(k)} - \underline{\boldsymbol{\mu}}_f^{(k)}) \geq \mathbf{0} \quad (3.5b)$$

$$\left. \begin{aligned} \gamma_f^{(k)} \boldsymbol{\Delta}_f^{(k)} + \mathbf{B}(\bar{\boldsymbol{\mu}}_f^{(k)} - \underline{\boldsymbol{\mu}}_f^{(k)}) &\geq \mathbf{0} \\ 0 \leq \gamma_f^{(k)} &\leq \frac{1}{(1 - \alpha_f)k_f} \\ \bar{\boldsymbol{\mu}}_f^{(k)} &\geq \mathbf{0}, \quad \underline{\boldsymbol{\mu}}_f^{(k)} \geq \mathbf{0} \end{aligned} \right\} \forall k \in K_f \quad (3.5c)$$

$$\left\| \sum_{k \in K_f} (\bar{\boldsymbol{\mu}}_f^{(k)} + \underline{\boldsymbol{\mu}}_f^{(k)}) \right\|_p \leq \frac{1}{1 - \alpha_f} \varepsilon_f \quad (3.5d)$$

$$\sum_{k \in K_f} \gamma_f^{(k)} = 1 \quad (3.5e)$$

$$\boldsymbol{\beta}_f \geq \mathbf{0}. \quad (3.5f)$$

Proof. See Supplementary Material A. \square

Theorem 1. *If the conditions of Lemma 1 are satisfied, then the basic DRI problem [DRI] admits the following single-level reformulation:*

$$\hat{z}_b^* = \min_{\mathbf{x}, \mathbf{y}, \boldsymbol{\nu}, \mathbf{s}, \boldsymbol{\mu}, \boldsymbol{\beta}, \boldsymbol{\gamma}, \lambda, t} \left\{ t_l + \frac{1}{1 - \alpha_l} (\varepsilon_l \lambda_l + \frac{1}{k_l} \sum_{k \in K_l} s_l^{(k)}) \right\} \quad (3.6a)$$

$$\text{s.t. } \mathbf{x} \in X \quad (3.6b)$$

$$\left. \begin{aligned} \hat{\mathbf{c}}_l^{(k)\top} \mathbf{y} - t_l + \boldsymbol{\Delta}_l^{(k)\top} \boldsymbol{\nu}_l^{(k)} &\leq s_l^{(k)} \\ \|\mathbf{B}^\top \boldsymbol{\nu}_l^{(k)} - \mathbf{y}\|_q &\leq \lambda_l \\ \boldsymbol{\nu}_l^{(k)} &\geq \mathbf{0}, s_l^{(k)} \geq 0 \end{aligned} \right\} \forall k \in K_l \quad (3.6c)$$

$$(3.4b)-(3.4d), (3.5b)-(3.5f) \quad (3.6d)$$

$$(-\mathbf{L}\mathbf{x} + \mathbf{f})^\top \boldsymbol{\beta}_f = t_f - \frac{1}{1 - \alpha_f} (\varepsilon_f \lambda_f + \frac{1}{k_f} \sum_{k \in K_f} s_f^{(k)}), \quad (3.6e)$$

where $\boldsymbol{\Delta}_l^{(k)} = \mathbf{b} - \mathbf{B}\hat{\mathbf{c}}_l^{(k)} \geq \mathbf{0}$ for each $k \in K_l$ and $\frac{1}{p} + \frac{1}{q} = 1$.

Proof. See Supplementary Material A. \square

As argued in [52], replacing the complementary slackness constraints by a single quadratic constraint (3.6e) has the potential to accelerate the computational complexity of the resulting single-level problem. At the same time, the single-level reformulation (3.6) contains a product of continuous dual variables, $\boldsymbol{\beta}_f$, and binary decision variables, \mathbf{x} . This product can be linearized using standard Big-M constraints, yielding a single-level MILP reformulation of [DRI]; see, e.g., [52]. As the choice of Big-M depends on the underlying problem's structure, we provide a detailed linearization approach along with specific test instances in Section 6.

3.2. Convergence analysis

Next, we analyze a relation between [DRI] and the respective full information model [SI], as the sample sizes of the leader and the follower tend to infinity. Our results are consistent with the standard asymptotic findings for one-stage Wasserstein DRO problems [25], reinforcing that [DRI] serves as a valid approximation of [SI]. To establish our convergence results, we introduce the following additional assumption:

A4. For given numbers of samples, k_l and k_f , and significance levels, $\theta_{k_l} \in (0, 1)$ and $\theta_{k_f} \in (0, 1)$, the Wasserstein radii, $\varepsilon_l(\theta_{k_l})$ and $\varepsilon_f(\theta_{k_f})$, can be selected so that the true distribution \mathbb{Q}^* belongs to \mathcal{Q}_l and \mathcal{Q}_f , respectively, with probabilities of at least $1 - \theta_{k_l}$ and $1 - \theta_{k_f}$. Moreover, let

$$\sum_{k_i=1}^{\infty} \theta_{k_i} < \infty \quad \text{and} \quad \lim_{k_i \rightarrow \infty} \varepsilon_i(\theta_{k_i}) = 0 \quad \forall i \in \{l, f\}.$$

Assumption **A4** is supported by standard measure concentration results for the Wasserstein distance and is essential for the convergence of one-stage Wasserstein DRO models; see Theorem 3.6 in [25]. In our setting, due to a similar structure of the leader's and the follower's ambiguity sets, the conditions of Assumption **A4** are simply reiterated for both decision-makers. Also, in the remainder of this section, $\mathbb{Q}^{*\infty}$ denotes the limiting distribution of the sample's behavior, as the sample size approaches infinity; recall our notations at the end of Section 1.2.

We begin with analyzing the follower's problem in **[DRI]** for a fixed leader's decision $\mathbf{x} \in X$. Thus, by leveraging the minimax theorem (see, e.g., Example 3 in [22]), the follower's problem in (3.1c) can be expressed as:

$$\hat{z}_f^*(\mathbf{x}, \hat{\mathbf{C}}_f) := \max_{\bar{\mathbf{y}} \in \bar{Y}(\mathbf{x})} \min_{\mathbb{Q}_f \in \mathcal{Q}_f} \mathbb{E}_{\mathbb{Q}_f} \{h_f(\mathbf{y}, t_f, \mathbf{c})\}, \quad (3.7)$$

where $\bar{\mathbf{y}} := (\mathbf{y}, t_f)$,

$$h_f(\mathbf{y}, t_f, \mathbf{c}) := t_f + \frac{1}{1 - \alpha_f} (\mathbf{c}^\top \mathbf{y} - t_f)^- \quad \text{and} \quad \bar{Y}(\mathbf{x}) := Y(\mathbf{x}) \times [\underline{t}_f, \bar{t}_f]$$

for some appropriate \underline{t}_f and \bar{t}_f . In particular, compactness of the sets X , $Y(\mathbf{x})$ and S , which is guaranteed by Assumptions **A1** and **A2**, yields that any optimal t_f^* in (3.2b) is such that:

$$-\infty < \underline{t}_f := \min_{\mathbf{x} \in X} \min_{(\mathbf{c}, \mathbf{y}) \in S \times Y(\mathbf{x})} \mathbf{c}^\top \mathbf{y} \leq t_f^* \leq \bar{t}_f := \max_{\mathbf{x} \in X} \max_{(\mathbf{c}, \mathbf{y}) \in S \times Y(\mathbf{x})} \mathbf{c}^\top \mathbf{y} < +\infty.$$

The following result establishes convergence for the follower.

Lemma 2. *Let $\mathbf{x} \in X$ be fixed and Assumptions **A1-A4** hold. Then, $\mathbb{Q}^{*\infty}$ -almost surely the follower's optimal objective function value in (3.7) satisfies*

$$\liminf_{k_f \rightarrow \infty} \hat{z}_f^*(\mathbf{x}, \hat{\mathbf{C}}_f) = z_f^*(\mathbf{x}) := \max_{\bar{\mathbf{y}} \in \bar{Y}(\mathbf{x})} \mathbb{E}_{\mathbb{Q}^*} \{h_f(\mathbf{y}, t_f, \mathbf{c})\}. \quad (3.8)$$

Furthermore, if $\bar{\mathbf{y}}^*(k_f)$ is an optimal solution of the follower's problem in (3.7), then $\mathbb{Q}^{*\infty}$ -almost surely any accumulation point of $\{\bar{\mathbf{y}}^*(k_f)\}_{k_f \in \mathbb{N}}$ is an optimal solution of the full information problem in (3.8).

Proof. Since $\bar{Y}(\mathbf{x})$ and S are compact, we conclude that $h_f(\mathbf{y}, t_f, \mathbf{c})$ is continuous and bounded uniformly for all feasible \mathbf{y} , t_f and \mathbf{c} . As $Y(\mathbf{x})$ is also closed, the result follows from Theorem 3.6 in [25]. \square

Next, analogously to the follower's problem, we formulate the leader's problem in **[DRI]** as:

$$\hat{z}_l^*(\hat{\mathbf{C}}_l, \hat{\mathbf{C}}_f) := \min_{\bar{\mathbf{x}} \in \bar{X}(\hat{\mathbf{C}}_f)} \max_{\mathbb{Q}_l \in \mathcal{Q}_l} \mathbb{E}_{\mathbb{Q}_l} \{h_l(\mathbf{y}, t_l, \mathbf{c})\}, \quad (3.9)$$

where $\bar{\mathbf{x}} := (\mathbf{x}, \mathbf{y}, t_l)$, $h_l(\mathbf{y}, t_l, \mathbf{c}) := t_l + \frac{1}{1 - \alpha_l} (\mathbf{c}^\top \mathbf{y} - t_l)^+$ and

$$\bar{X}(\hat{\mathbf{C}}_f) := \left\{ (\mathbf{x}, \bar{\mathbf{y}}, t_l) : \mathbf{x} \in X, \bar{\mathbf{y}} = (\mathbf{y}, t_f) \in \hat{V}_f(\mathbf{x}, \hat{\mathbf{C}}_f), t_l \in [\underline{t}_l, \bar{t}_l] \right\}. \quad (3.10)$$

Specifically, we define $\underline{t}_l := \underline{t}_f$, $\bar{t}_l := \bar{t}_f$ and

$$\hat{V}_f(\mathbf{x}, \hat{\mathbf{C}}_f) := \operatorname{argmax}_{(\tilde{\mathbf{y}}, \tilde{t}_f) \in \bar{Y}(\mathbf{x})} \left\{ \min_{\mathbf{c} \in \mathcal{Q}_f} \mathbb{E}_{\mathbb{Q}_f} \{h_f(\tilde{\mathbf{y}}, \tilde{t}_f, \mathbf{c})\} \right\}. \quad (3.11)$$

To establish convergence for the leader, we need to make the following additional assumption:

A5. For every fixed $\mathbf{x} \in X$, the full information follower's problem

$$\max_{\bar{\mathbf{y}} \in \bar{Y}(\mathbf{x})} \mathbb{E}_{\mathbb{Q}^*} \{h_f(\mathbf{y}, t_f, \mathbf{c})\}, \quad (3.12)$$

where $\bar{\mathbf{y}} = (\mathbf{y}, t_f)$, has a unique optimal solution.

Assumption **A5** is often used for deriving theoretical properties of bilevel optimization problems; see, e.g., [23]. Some additional limitations related to Assumption **A5** are discussed later, after presenting the proof of our convergence result.

Lemma 3. *Let*

$$v_f(\mathbf{y}, \hat{\mathbf{C}}_f) := \min_{\mathbf{Q}_f \in \mathcal{Q}_f(\hat{\mathbf{C}}_f)} \rho_f(\mathbf{y}, \mathbf{Q}_f) \text{ and } \hat{V}_f(\mathbf{x}, \hat{\mathbf{C}}_f) := \operatorname{argmax}_{\tilde{\mathbf{y}} \in \bar{Y}(\mathbf{x})} v_f(\tilde{\mathbf{y}}, \hat{\mathbf{C}}_f)$$

be the follower's optimal objective function value and the corresponding optimal solution set in (3.11). Then, for any fixed $\mathbf{x} \in X$, $v_f(\mathbf{y}, \hat{\mathbf{C}}_f)$ is continuous in both \mathbf{y} and $\hat{\mathbf{C}}_f$, and $\hat{V}_f(\mathbf{x}, \hat{\mathbf{C}}_f)$ is non-empty and upper semicontinuous in $\hat{\mathbf{C}}_f$.

Proof. See Supplementary Material A. □

Theorem 2. *Let Assumptions **A1-A5** hold. Then, $\mathbb{Q}^{*\infty}$ -almost surely the leader's optimal objective function value in (3.9) satisfies*

$$\limsup_{k_f \rightarrow \infty} \limsup_{k_l \rightarrow \infty} \hat{z}_l^*(\hat{\mathbf{C}}_l, \hat{\mathbf{C}}_f) = z^* := \min_{\bar{\mathbf{x}} \in \bar{X}^*} \mathbb{E}_{\mathbb{Q}^*} \{h_l(\mathbf{y}, t_l, \mathbf{c})\}, \quad (3.13)$$

where z^ is the optimal objective function value of the stochastic programming problem [SP], with*

$$\bar{X}^* := \left\{ (\mathbf{x}, \bar{\mathbf{y}}, t_l) : \mathbf{x} \in X, \bar{\mathbf{y}} = (\mathbf{y}, t_f) \in V_f^*(\mathbf{x}), t_l \in [\underline{t}_l, \bar{t}_l] \right\} \text{ and} \quad (3.14)$$

$$V_f^*(\mathbf{x}) := \operatorname{argmax}_{(\mathbf{y}, t_f) \in \bar{Y}(\mathbf{x})} \mathbb{E}_{\mathbb{Q}^*} \{h_f(\mathbf{y}, t_f, \mathbf{c})\}. \quad (3.15)$$

Furthermore, if $\bar{\mathbf{x}}^(k_l, k_f)$ is an optimal solution of the leader's problem in (3.9), then $\mathbb{Q}^{*\infty}$ -almost surely any accumulation point of $\{\bar{\mathbf{x}}^*(k_l, k_f)\}_{k_l, k_f \in \mathbb{N}}$ is an optimal solution of the full information problem in (3.13).*

Proof. Let the follower's sample size, k_f , and its data set, $\hat{\mathbf{C}}_f$, be fixed. Additionally, based on Assumption **A3**, we also fix the first k_f samples in the leader's data set, $\hat{\mathbf{C}}_l$. It is important to note, however, that fixing a finite number of samples in the leader's data set does not impact our convergence results, since we focus only on asymptotic performance guarantees for the leader.

Closedness of $\bar{X}(\hat{\mathbf{C}}_f)$. Initially, we demonstrate that Theorem 3.6 in [25] can also be applied to the leader's problem in (3.9). Similar to the proof of Lemma 2, we observe that $h_l(\mathbf{y}, t_l, \mathbf{c})$ is continuous and bounded uniformly for all feasible \mathbf{y} , t_l and \mathbf{c} . Thus, it suffices to show that the leader's feasible set $\bar{X}(\hat{\mathbf{C}}_f)$ given by equation (3.10) is closed. Let $\bar{\mathbf{x}}(k) = (\mathbf{x}, \mathbf{y}, t_f, t_l) \in \bar{X}(\hat{\mathbf{C}}_f)$ be a sequence of points such that

$$\lim_{k \rightarrow \infty} \bar{\mathbf{x}}(k) = \bar{\mathbf{x}}^{\text{lim}} = (\mathbf{x}^{\text{lim}}, \mathbf{y}^{\text{lim}}, t_f^{\text{lim}}, t_l^{\text{lim}});$$

for simplicity, the dependence on k is omitted in the notation whenever it is clear from the context. Since X is a discrete set, it can be observed that $\mathbf{x}^{\text{lim}} \in X$ and, furthermore, there exists $k_0 \in \mathbb{N}$ such that for all $k \geq k_0$ we have $\mathbf{x}(k) = \mathbf{x}^{\text{lim}}$. Also, $t_l^{\text{lim}} \in [\underline{t}_l, \bar{t}_l]$ and, to verify that $\bar{X}(\hat{\mathbf{C}}_f)$ is closed, we only need to check that

$$\bar{\mathbf{y}}^{\text{lim}} = (\mathbf{y}^{\text{lim}}, t_f^{\text{lim}}) \in \hat{V}_f(\mathbf{x}^{\text{lim}}, \hat{\mathbf{C}}_f), \quad (3.16)$$

given that

$$\bar{\mathbf{y}}(k) = (\mathbf{y}, t_f) \in \hat{V}_f(\mathbf{x}^{\text{lim}}, \hat{\mathbf{C}}_f) \quad \forall k \geq k_0.$$

The latter observation follows from the closedness of the optimal solution set $\hat{V}_f(\mathbf{x}^{\text{lim}}, \hat{\mathbf{C}}_f)$. Indeed, by Lemma 3, the follower's objective function in (3.11) is continuous and $\hat{V}_f(\mathbf{x}^{\text{lim}}, \hat{\mathbf{C}}_f)$ is non-empty. Therefore, $\bar{\mathbf{y}}(k)$, $k \geq k_0$, and $\bar{\mathbf{y}}^{\text{lim}}$ provide the same optimal objective function value for the follower and the relation (3.16) holds.

As a result, Theorem 3.6 in [25] implies that $\mathbb{Q}^{*\infty}$ -almost surely

$$\limsup_{k_l \rightarrow \infty} \hat{z}^*(\hat{\mathbf{C}}_l, \hat{\mathbf{C}}_f) = \hat{z}^*(\hat{\mathbf{C}}_f) = \min_{(\mathbf{x}, \bar{\mathbf{y}}, t_l) \in \bar{X}(\hat{\mathbf{C}}_f)} \mathbb{E}_{\mathbb{Q}^*} \{h_l(\mathbf{y}, t_l, \mathbf{c})\}. \quad (3.17)$$

Also, given an optimal solution $\bar{\mathbf{x}}^*(k_l, k_f) := (\hat{\mathbf{x}}^*, \hat{\mathbf{y}}^*, \hat{t}_f^*, \hat{t}_l^*)$ of the leader's problem (3.9), any accumulation point

$$\bar{\mathbf{x}}^*(k_f) := (\tilde{\mathbf{x}}^*, \tilde{\mathbf{y}}^*, \tilde{t}_f^*, \tilde{t}_l^*) \quad (3.18)$$

of the sequence $\{\bar{\mathbf{x}}^*(k_l, k_f)\}_{k_l \in \mathbb{N}}$ is an optimal solution of (3.17).

Feasibility of $\bar{\mathbf{x}}^$.* Next, we consider an accumulation point

$$\bar{\mathbf{x}}^* = (\mathbf{x}^*, \mathbf{y}^*, t_f^*, t_l^*) \quad (3.19)$$

of the sequence $\{\bar{\mathbf{x}}^*(k_f)\}_{k_f \in \mathbb{N}}$, as k_f tends to infinity; this point is essentially an accumulation point of the double-indexed sequence $\{\bar{\mathbf{x}}^*(k_l, k_f)\}_{k_l, k_f \in \mathbb{N}}$ by construction. Our goal is to show that

$$\limsup_{k_f \rightarrow \infty} \hat{z}^*(\hat{\mathbf{C}}_f) = z^* = \min_{(\mathbf{x}, \bar{\mathbf{y}}, t_l) \in \bar{X}^*} \mathbb{E}_{\mathbb{Q}^*} \{h_l(\mathbf{y}, t_l, \mathbf{c})\}, \quad (3.20)$$

where $\hat{z}^*(\hat{\mathbf{C}}_f)$ is defined by equation (3.17), and that $\bar{\mathbf{x}}^*$ is an optimal solution of the full information problem in the right-hand side of (3.20).

We first prove that $\bar{\mathbf{x}}^*$ is feasible in (3.20), i.e., $\bar{\mathbf{x}}^* \in \bar{X}^*$, where \bar{X}^* is defined by equation (3.14).

By passing to a subsequence, if necessary, let

$$\lim_{k_f \rightarrow \infty} \bar{\mathbf{x}}^*(k_f) = \bar{\mathbf{x}}^*.$$

By similar reasoning as for the closedness of $\bar{X}(\hat{\mathbf{C}}_f)$, we conclude that $t_l^* \in [\underline{t}_l, \bar{t}_l]$ and there exists $k_0 \in \mathbb{N}$ such that for all $k_f \geq k_0$, we have $\tilde{\mathbf{x}}^*(k_f) = \mathbf{x}^* \in X$; recall definitions (3.18) and (3.19). Assuming that $k_f \geq k_0$ and, therefore, $\tilde{\mathbf{x}}^*(k_f) = \mathbf{x}^*$, Lemma 2 implies that

$$\bar{\mathbf{y}}^* = (\mathbf{y}^*, t_f^*) = \lim_{k_f \rightarrow \infty} (\tilde{\mathbf{y}}^*(k_f), \tilde{t}_f^*(k_f))$$

is an optimal solution of the full information follower's problem

$$\max_{\bar{\mathbf{y}}^* \in Y(\mathbf{x}^*)} \mathbb{E}_{\mathbb{Q}^*} \{h_f(\mathbf{y}, t_f, \mathbf{c})\},$$

and, therefore, $\bar{\mathbf{x}}^*$ is feasible in (3.20), i.e., $\bar{\mathbf{x}}^* \in \bar{X}^*$.

Upper bound. In order to prove the equality in (3.20), we first prove that

$$\limsup_{k_f \rightarrow \infty} \hat{z}^*(\hat{\mathbf{C}}_f) \geq z^*.$$

Indeed, given a sequence $\{\bar{\mathbf{x}}^*(k_f)\}_{k_f \in \mathbb{N}}$ and its accumulation point $\bar{\mathbf{x}}^* \in \bar{X}^*$ defined by equations (3.18) and (3.19), respectively, we observe that

$$\begin{aligned} \lim_{k_f \rightarrow \infty} \hat{z}^*(\hat{\mathbf{C}}_f) &= \lim_{k_f \rightarrow \infty} \mathbb{E}_{\mathbb{Q}^*} \{h_l(\tilde{\mathbf{y}}^*(k_f), \tilde{t}_l^*(k_f), \mathbf{c})\} = \\ \mathbb{E}_{\mathbb{Q}^*} \left\{ \lim_{k_f \rightarrow \infty} h_l(\tilde{\mathbf{y}}^*(k_f), \tilde{t}_l^*(k_f), \mathbf{c}) \right\} &= \mathbb{E}_{\mathbb{Q}^*} \{h_l(\mathbf{y}^*, t_l^*, \mathbf{c})\} \geq z^*. \end{aligned} \tag{3.21}$$

Here, the first equality follows from the fact that $\bar{\mathbf{x}}^*(k_f)$ is an optimal solution of (3.17). The second equality is due to the bounded convergence theorem [3], which holds since $h_l(\mathbf{y}, t_l, \mathbf{c})$ is continuous and uniformly bounded. Furthermore, the third equality and the last inequality hold since $h_l(\mathbf{y}, t_l, \mathbf{c})$ is continuous and $\bar{\mathbf{x}}^* \in \bar{X}^*$, respectively.

Lower bound. As a result, it remains to show that

$$\limsup_{k_f \rightarrow \infty} \hat{z}^*(\hat{\mathbf{C}}_f) \leq z^*.$$

By definition of the minimum in (3.17), we have

$$\hat{z}^*(\hat{\mathbf{C}}_f) \leq \mathbb{E}_{\mathbb{Q}^*} \{h_l(\mathbf{y}, t_l, \mathbf{c})\} \quad \forall (\mathbf{x}, \bar{\mathbf{y}}, t_l) \in \bar{X}(\hat{\mathbf{C}}_f). \tag{3.22}$$

Let $\bar{\mathbf{x}}^0 = (\mathbf{x}^0, \mathbf{y}^0, t_f^0, t_l^0)$ be an optimal solution of the full information problem in (3.13). The main challenge is that there is no guarantee that $\bar{\mathbf{x}}^0 \in \bar{X}(\hat{\mathbf{C}}_f)$. For this reason, we define the right-hand

side of (3.22) with $\mathbf{x} := \mathbf{x}^0$, $t_l := t_l^0$ and an *arbitrary* point

$$\bar{\mathbf{y}}^0(k_f) := (\tilde{\mathbf{y}}^0, \tilde{t}_f^0) \in \hat{V}_f(\mathbf{x}^0, \hat{\mathbf{C}}_f). \quad (3.23)$$

where $\hat{V}_f(\mathbf{x}^0, \hat{\mathbf{C}}_f)$ is non-empty by Lemma 3.

Next, by design, we have

$$\bar{\mathbf{x}}^0(k_f) := (\mathbf{x}^0, \tilde{\mathbf{y}}^0, \tilde{t}_f^0, t_l^0) \in \bar{X}(\hat{\mathbf{C}}_f)$$

and, therefore, (3.22) yields that

$$\hat{z}^*(\hat{\mathbf{C}}_f) \leq \mathbb{E}_{\mathbb{Q}^*} \{h_l(\tilde{\mathbf{y}}^0(k_f), t_l^0, \mathbf{c})\}. \quad (3.24)$$

Also, by Lemma 2 and Assumption **A5**, any accumulation point of the sequence $\{\bar{\mathbf{y}}^0(k_f)\}_{k_f \in \mathbb{N}}$ defined by equation (3.23) is given by (\mathbf{y}^0, t_f^0) . Given that the latter sequence is bounded, we conclude that

$$\lim_{k_f \rightarrow \infty} \bar{\mathbf{y}}^0(k_f) = (\mathbf{y}^0, t_f^0),$$

where the limit is understood with respect to all convergent subsequences.

By using the same argument as in (3.21), we observe that

$$\lim_{k_f \rightarrow \infty} \mathbb{E}_{\mathbb{Q}^*} \{h_l(\tilde{\mathbf{y}}^0(k_f), t_l^0, \mathbf{c})\} = \mathbb{E}_{\mathbb{Q}^*} \left\{ \lim_{k_f \rightarrow \infty} h_l(\tilde{\mathbf{y}}^0(k_f), t_l^0, \mathbf{c}) \right\} = \mathbb{E}_{\mathbb{Q}^*} \{h_l(\mathbf{y}^0, t_l^0, \mathbf{c})\} = z^*.$$

By applying the limit superior to both sides of (3.24), we have:

$$\limsup_{k_f \rightarrow \infty} \hat{z}^*(\hat{\mathbf{C}}_f) \leq \limsup_{k_f \rightarrow \infty} \mathbb{E}_{\mathbb{Q}^*} \{h_l(\tilde{\mathbf{y}}^0, t_l^0, \mathbf{c})\} = z^*. \quad (3.25)$$

Therefore, taking into account (3.21), we conclude that $\limsup_{k_f \rightarrow \infty} \hat{z}^*(\hat{\mathbf{C}}_f) = z^*$. Finally, equations (3.21) and (3.25) imply that

$$z^* \geq \limsup_{k_f \rightarrow \infty} \hat{z}^*(\hat{\mathbf{C}}_f) \geq \lim_{k_f \rightarrow \infty} \hat{z}^*(\hat{\mathbf{C}}_f) = \mathbb{E}_{\mathbb{Q}^*} \{h_l(\mathbf{y}^*, t_l^*, \mathbf{c})\} \geq z^*,$$

which means that $\bar{\mathbf{x}}^* = (\mathbf{x}^*, \mathbf{y}^*, t_l^*, t_f^*)$ is an optimal solution of (3.13). This observation concludes the proof. \square

Notably, in the formulation of Theorem 2, our focus is on the limit superior, as the leader minimizes its objective function in (3.9) with respect to all feasible values of \mathbf{x} and \mathbf{y} and, therefore, convergence in terms of the worst-case upper bound is of main interest. Furthermore, the proof of Theorem 2 exploits discreteness of the leader's feasible set X and uniqueness of a solution to the full information follower's problem (3.12); recall Assumption **A5**.

Admittedly, **A5** cannot be verified in practice, since the true distribution \mathbb{Q}^* is not known. However, even if Assumption **A5** is violated, equation (3.21) shows that the leader's optimal objective function value in **[DRI]** converges to an upper bound of the true optimal objective function value, z^* .

This observation suggests that, even though we consider an optimistic version of **[DRI]**, it may offer a more conservative approach from the leader’s perspective compared to **[SI]**.

4. Pessimistic approximation

4.1. Problem formulation and complexity

In line with Example 1, to relax Assumption **A3**, we consider a *true basic model* given by:

$$[\mathbf{DRI}^*]: \quad z_b^* := \min_{\mathbf{x}, \mathbf{y}} \left\{ \max_{\mathbb{Q}_l \in \mathcal{Q}_l} \rho_l(\mathbf{y}, \mathbb{Q}_l) \right\} \quad (4.1a)$$

$$\text{s.t. } \mathbf{x} \in X \quad (4.1b)$$

$$\mathbf{y} \in \operatorname{argmax}_{\tilde{\mathbf{y}} \in Y(\mathbf{x})} \left\{ \min_{\mathbb{Q}_f \in \mathcal{Q}_f(\hat{\mathbf{C}}_f^*)} \rho_f(\tilde{\mathbf{y}}, \mathbb{Q}_f) \right\}, \quad (4.1c)$$

where $\hat{\mathbf{C}}_f^*$ denotes the true follower’s data set. In essence, **[DRI]** and **[DRI*]** are identical problems. However, in the true basic model **[DRI*]**, we do not assume that the follower’s data set is a subset of the leader’s, i.e., the second part of Assumption **A3** does not hold. We emphasize that **[DRI*]** is a *hypothetical* model, as whenever the leader has access to $\hat{\mathbf{C}}_f^*$, it should also incorporate this data into its own data set.

We begin by proposing a *pessimistic approximation* of the true basic model **[DRI*]**; recall case (i) in Example 1. Formally, the pessimistic approximation can be formulated as:

$$[\mathbf{DRI-P}]: \quad \hat{z}_p^* := \min_{\mathbf{x} \in X} \max_{\mathbf{y} \in Y(\mathbf{x})} \max_{\mathbb{Q}_l \in \mathcal{Q}_l} \rho_l(\mathbf{y}, \mathbb{Q}_l), \quad (4.2)$$

where $\rho_l(\mathbf{y}, \mathbb{Q}_l)$ is defined by equation (3.2a). That is, the leader in **[DRI-P]** disregards any available information about the true follower’s data set $\hat{\mathbf{C}}_f^*$ and selects the worst-case *feasible* follower’s policy in terms of the leader’s objective function value.

In view of case (ii) in Example 1, we conclude that the pessimistic approximation **[DRI-P]** can be rather conservative, potentially providing a wrong estimate of the true follower’s policy. In addition, assuming that the support set S is not necessarily compact, we prove that **[DRI-P]** is Σ_2^P -hard. Notably, while Assumption **A2** requires S to be compact, more general Wasserstein DRO models allow unbounded support sets [25, 26]. The following result holds.

Theorem 3. *Let Assumption **A1** hold and assume that the support set S defined by equation (2.3) is not necessarily compact. Then, the pessimistic approximation **[DRI-P]** is Σ_2^P -hard.*

Proof. We show Σ_2^P -hardness by a reduction from the dominating set interdiction problem [27].

Given an undirected graph $G = (V, E)$, a *dominating set* is a subset of vertices $D \subseteq V$ such that every vertex $v \in V$ is either in D or adjacent to at least one vertex in D . That is, for every $v \in V$, either $v \in D$ or there exists $u \in D$ such that $(u, v) \in E$. A decision version of the dominating set interdiction (DSI-D) problem can be formulated as follows:

[DSI-D]: Given an undirected graph $G = (V, E)$, a threshold $t \in \mathbb{Z}_+$, and a budget $b \in \mathbb{Z}_+$, is there a subset of vertices $B \subseteq V$ with $|B| \leq b$ such that there is no dominating set $D \subseteq V \setminus B$ with size $\leq t$?

Importantly, **[DSI-D]** is proved to be Σ_2^P -complete; see Theorems 15 and 37 in [27].

Next, we introduce the following three-level problem:

$$\tilde{z}^* = \min_{\mathbf{x} \in \tilde{X}} \max_{\mathbf{y} \in \tilde{Y}(\mathbf{x})} \min_{\mathbf{z} \in \tilde{Z}(\mathbf{y})} - \sum_{i \in V} z_i, \quad (4.3)$$

where $\tilde{X} = \{\mathbf{x} \in \{0, 1\}^{|V|} : \sum_{i \in V} x_i \leq b\}$,

$$\tilde{Y}(\mathbf{x}) = \left\{ \mathbf{y} \in \{0, 1\}^{|V|} : y_i \leq 1 - x_i \quad \forall i \in V, \quad \sum_{i \in V} y_i \leq t \right\} \text{ and} \quad (4.4a)$$

$$\tilde{Z}(\mathbf{y}) = \left\{ \mathbf{z} \in \mathbb{R}_+^{|V|} : z_i \leq 1 - y_i \quad \forall i \in V, \quad z_i \leq 1 - y_j \quad \forall (i, j) \in E \right\}. \quad (4.4b)$$

We demonstrate that **[DSI-D]** admits a “yes”-instance if and only if $\tilde{z}^* < 0$. Indeed, if the answer to **[DSI-D]** is “yes”, then we can select $x_i = 1$ for $i \in B$ and $x_i = 0$ otherwise. Then, since there are no dominating sets of size $\leq t$ in the residual graph, for any $\mathbf{y} \in \tilde{Y}(\mathbf{x})$, we can identify at least one non-dominated vertex $i \in V$ such that $z_i^* = 1$. Hence, $\tilde{z}^* < 0$.

Conversely, assume that $\tilde{z}^* < 0$ but the answer to **[DSI-D]** is “no”. Then, for any $B \subseteq V$, $|B| \leq b$, there exists a dominating set of size $\leq t$ in the residual graph. In other words, for any $\mathbf{x} \in \tilde{X}$, there exists $\mathbf{y} \in \tilde{Y}(\mathbf{x})$ such that $\tilde{Z}(\mathbf{y}) = \{\mathbf{0}\}$. This contradicts the assumption that $\tilde{z}^* < 0$.

Finally, we show that (4.3) reduces to an instance of **[DRI-P]** with $\alpha_l = 0$ and $\varepsilon_l = \infty$, i.e.,

$$\hat{z}_p^* = \min_{\mathbf{x} \in X} \max_{\mathbf{y} \in Y(\mathbf{x})} \max_{\mathbf{c} \in S} \mathbf{c}^\top \mathbf{y}. \quad (4.5)$$

Let $\boldsymbol{\beta} \in \mathbb{R}_+^{|V|}$ and $\boldsymbol{\gamma} \in \mathbb{R}_+^{|E|}$ be dual variables corresponding to the vertex-based and the edge-based constraints in (4.4b). Then, (4.3) admits an equivalent single-level dual reformulation given by:

$$\min_{\mathbf{x} \in \tilde{X}} \max_{\mathbf{y}, \boldsymbol{\beta}, \boldsymbol{\gamma}} \sum_{j \in V} \left(\beta_j + \sum_{i: (i, j) \in E} \gamma_{ij} \right) (y_j - 1) \quad (4.6a)$$

$$\text{s.t. } \mathbf{y} \in \tilde{Y}(\mathbf{x}) \quad (4.6b)$$

$$\beta_j + \sum_{i: (i, j) \in E} \gamma_{ij} \geq 1 \quad \forall j \in V \quad (4.6c)$$

$$\boldsymbol{\gamma}, \boldsymbol{\beta} \geq \mathbf{0}. \quad (4.6d)$$

Next, for each $j \in V$, we set $y'_j := 1 - y_j$ and

$$\delta_j := -\beta_j - \sum_{i: (i, j) \in E} \gamma_{ij}.$$

As a result, (4.6) reads as:

$$\min_{\mathbf{x} \in \tilde{X}} \max_{\mathbf{y}', \boldsymbol{\beta}, \boldsymbol{\gamma}, \boldsymbol{\delta}} \boldsymbol{\delta}^\top \mathbf{y}' \quad (4.7a)$$

$$\text{s.t. } \mathbf{x} \leq \mathbf{y}' \leq \mathbf{1} \quad (4.7b)$$

$$\sum_{i \in V} y'_i \geq |V| - t \quad (4.7c)$$

$$\delta_j = -\beta_j - \sum_{i: (i,j) \in E} \gamma_{ij} \quad \forall j \in V \quad (4.7d)$$

$$\delta_j \leq -1 \quad \forall j \in V \quad (4.7e)$$

$$\boldsymbol{\gamma}, \boldsymbol{\beta} \geq \mathbf{0}. \quad (4.7f)$$

In particular, the integrality constraints for \mathbf{y}' can be relaxed, since the objective function in (4.7) is bilinear and constraints (4.7b)-(4.7c) define an integral polytope.

We conclude that (4.7) is a special case of (4.5). Specifically, constraints (4.7b)-(4.7c) are associated with the follower's feasible set in (4.5), which is non-empty and compact by design. On the other hand, constraints (4.7d)-(4.7f) describe an unbounded support set. This observation concludes the proof. \square

Based on Theorem 3, we conclude that, even for the risk-neutral leader, the pessimistic approximation **[DRI-P]** is Σ_2^p -hard. In the following, we focus on two special cases of the problem, where the leader is either ambiguity-free ($\varepsilon_l = 0$) or risk-neutral ($\alpha_l = 0$). In these cases, the second-level problem in **[DRI-P]** reduces to a bilinear problem with disjoint constraints. Then, under some additional assumptions, both versions of **[DRI-P]** can be solved using a specialized Benders decomposition algorithm, combined with taking a partial dual of the second-level problem; see, e.g., [53]. The following result provides a general reformulation of **[DRI-P]** for a fixed $\mathbf{x} \in X$.

Theorem 4. *Let Assumptions **A1**, **A2** and the first part of Assumption **A3** hold. If the leader's ambiguity set \mathcal{Q}_l is defined in terms of p -norm with $p \in \{1, \infty\}$, then, for any $\mathbf{x} \in X$, the second-level problem in **[DRI-P]** admits the following non-convex quadratic reformulation:*

$$\max_{\mathbf{y}, \boldsymbol{\xi}_l, \boldsymbol{\eta}_l, \boldsymbol{\gamma}_l} \left\{ \frac{1}{k_l(1 - \alpha_l)} \sum_{k \in K_l} (\gamma_l^{(k)} \hat{\mathbf{c}}_l^{(k)} - \boldsymbol{\xi}_l^{(k)})^\top \mathbf{y} \right\} \quad (4.8a)$$

$$\text{s.t. } \mathbf{y} \in Y(\mathbf{x}) \quad (4.8b)$$

$$\left. \begin{aligned} \mathbf{B}(\gamma_l^{(k)} \hat{\mathbf{c}}_l^{(k)} - \boldsymbol{\xi}_l^{(k)}) &\leq \gamma_l^{(k)} \mathbf{b} \\ 0 &\leq \gamma_l^{(k)} \leq 1 \\ -\boldsymbol{\eta}_l^{(k)} &\leq \boldsymbol{\xi}_l^{(k)} \leq \boldsymbol{\eta}_l^{(k)} \end{aligned} \right\} \forall k \in K_l \quad (4.8c)$$

$$\sum_{k \in K_l} \gamma_l^{(k)} = k_l(1 - \alpha_l) \quad (4.8d)$$

$$\left\| \frac{1}{k_l} \sum_{k \in K_l} \boldsymbol{\eta}_l^{(k)} \right\|_p \leq \varepsilon_l. \quad (4.8e)$$

Proof. See Supplementary Material A. \square

4.2. Benders decomposition-based algorithm for the ambiguity-free problem

First, we provide a reformulation of the pessimistic approximation **[DRI-P]** for the case of $\varepsilon_l = 0$.

Corollary 1. *Assume that the leader is ambiguity-free, i.e., $\varepsilon_l = 0$. Then, **[DRI-P]** reads as:*

$$\min_{\mathbf{x} \in X} \max_{\mathbf{y}, \gamma_l} \left\{ \frac{1}{k_l(1 - \alpha_l)} \sum_{k \in K_l} (\gamma_l^{(k)} \hat{\mathbf{c}}_l^{(k)})^\top \mathbf{y} \right\} \quad (4.9a)$$

$$\text{s.t. } \mathbf{y} \in Y(\mathbf{x}) \quad (4.9b)$$

$$0 \leq \gamma_l^{(k)} \leq 1 \quad \forall k \in K_l \quad (4.9c)$$

$$\sum_{k \in K_l} \gamma_l^{(k)} = k_l(1 - \alpha_l). \quad (4.9d)$$

Proof. The result readily follows by setting $\varepsilon_l = 0$ in the second-level problem reformulation (4.8). \square

Next, we make the following additional assumption:

A6. The leader's confidence level $\alpha_l \in (0, 1)$ is such that $k_l(1 - \alpha_l)$ is integer.

In fact, Assumption **A6** does not impose a significant restriction, since even if $k_l(1 - \alpha_l) \notin \mathbb{N}$, one may slightly perturb α_l or k_l to ensure that the integrality condition holds. First, we note that, under Assumption **A6**, the ambiguity-free problem (4.9) can be expressed as:

$$\min_{\mathbf{x}, z} z \quad (4.10a)$$

$$\text{s.t. } \mathbf{x} \in X \quad (4.10b)$$

$$z \geq \max_{\mathbf{y} \in Y(\mathbf{x})} \left\{ \bar{\mathbf{c}}(\gamma_l)^\top \mathbf{y} \right\} \quad \forall \gamma_l \in \Gamma, \quad (4.10c)$$

where $\bar{\mathbf{c}}(\gamma_l) := \frac{1}{k_l(1 - \alpha_l)} \sum_{k \in K_l} \gamma_l^{(k)} \hat{\mathbf{c}}_l^{(k)}$ and

$$\Gamma := \left\{ \gamma_l \in \{0, 1\}^{k_l} : \sum_{k \in K_l} \gamma_l^{(k)} = k_l(1 - \alpha_l) \right\}. \quad (4.11)$$

Indeed, the objective function (4.9a) is bilinear and constraints (4.9c)-(4.9d) define an integral polytope, whose extreme points are given by Γ .

Then, our algorithm closely follows the reformulation and linearization approach of Zeng and An [53] and the standard Benders decomposition approach of Israeli and Wood [29]; see Algorithm 1 for its pseudocode. First, by leveraging a dual reformulation of constraints (4.10c) for a given subset $\hat{\Gamma} \subseteq \Gamma$, we define a *master problem*

$$[\mathbf{MP}(\hat{\Gamma})] : \min_{\mathbf{x}, \beta, z} z \quad (4.12a)$$

$$\text{s.t. } \mathbf{x} \in X \quad (4.12b)$$

$$\left. \begin{aligned} z &\geq \beta(\gamma_l)^\top (\mathbf{f} - \mathbf{L}\mathbf{x}) \\ \beta(\gamma_l) &\geq \mathbf{0} \\ \mathbf{F}^\top \beta(\gamma_l) - \bar{\mathbf{c}}(\gamma_l) &\geq \mathbf{0} \end{aligned} \right\} \forall \gamma_l \in \hat{\Gamma} \quad (4.12c)$$

and a *subproblem*

$$[\mathbf{Sub}(\mathbf{x})] : \max_{\mathbf{y}, \gamma_l} \left\{ \bar{\mathbf{c}}(\gamma_l)^\top \mathbf{y} : \mathbf{y} \in Y(\mathbf{x}), \gamma_l \in \Gamma \right\}. \quad (4.13)$$

Notably, by Assumption **A1**, the primal problem in the right-hand side of (4.10c) has a finite optimum, ensuring that the optimal objective function value in $[\mathbf{MP}(\hat{\Gamma})]$ is finite. Furthermore, both $[\mathbf{MP}(\hat{\Gamma})]$ and $[\mathbf{Sub}(\mathbf{x})]$ admit single-level MILP reformulations, after applying standard linearization techniques to the products of continuous and binary decision variables.

Algorithm 1: A basic Benders decomposition-based algorithm for (4.9).

```

1 Input: the ambiguity-free problem (4.9) and a tolerance level  $\delta \in \mathbb{R}_+$ .
2 Output: an optimal solution  $\hat{\mathbf{x}}_p^* \in X$  and the optimal objective function value  $\hat{z}_p^*$ .
3  $LB \leftarrow -\infty, UB \leftarrow \infty$ 
4  $\hat{\mathbf{x}}^* \leftarrow \mathbf{0}, \hat{\Gamma} \leftarrow \emptyset$ 
5 while  $UB - LB > \delta$  do
6    $(\hat{\mathbf{y}}^*, \hat{\gamma}_l^*) \leftarrow$  an optimal solution of  $[\mathbf{Sub}(\hat{\mathbf{x}}^*)]$ 
7    $UB' \leftarrow$  the optimal objective function value of  $[\mathbf{Sub}(\hat{\mathbf{x}}^*)]$ 
8   if  $UB' < UB$  then
9      $(\hat{\mathbf{x}}_p^*, \hat{z}_p^*) \leftarrow (\hat{\mathbf{x}}^*, UB')$ 
10     $UB \leftarrow UB'$ 
11   end
12    $\hat{\Gamma} \leftarrow \hat{\Gamma} \cup \{\hat{\gamma}_l^*\}$ 
13    $(\hat{\mathbf{x}}^*, \hat{z}^*) \leftarrow$  an optimal solution of  $[\mathbf{MP}(\hat{\Gamma})]$ ,
14    $LB \leftarrow \hat{z}^*$ 
15 end
16 return  $\hat{\mathbf{x}}_p^*, \hat{z}_p^*$ 

```

Next, in lines 3–4 of Algorithm 1, we initialize the lower and the upper bounds, LB and UB , respectively, along with the initial set $\hat{\Gamma}$ and the leader’s interdiction decision $\hat{\mathbf{x}}^*$. In lines 5–14, the upper and the lower bounds are updated sequentially by solving the subproblem $[\mathbf{Sub}(\hat{\mathbf{x}}^*)]$ and the master problem $[\mathbf{MP}(\hat{\Gamma})]$, respectively. This process is repeated until LB and UB converge within a predefined tolerance δ . Overall, Algorithm 1 converges in a finite number of iterations since Γ is finite; see Proposition 8 in [53].

4.3. Benders decomposition-based algorithm for the risk-neutral problem

In this section, under some additional assumptions, we provide a similar algorithm for the risk-neutral pessimistic approximation $[\mathbf{DRI-P}]$. The following result presents a reformulation of $[\mathbf{DRI-P}]$

for the case of $\alpha_l = 0$.

Corollary 2. *Assume that the leader is risk-neutral, i.e., $\alpha_l = 0$. Then, [DRI-P] reads as:*

$$\min_{\mathbf{x} \in X} \max_{\mathbf{y}, \boldsymbol{\xi}_l, \boldsymbol{\eta}_l} \left\{ \frac{1}{k_l} \sum_{k \in K_l} (\hat{\mathbf{c}}_l^{(k)} - \boldsymbol{\xi}_l^{(k)})^\top \mathbf{y} \right\} \quad (4.14a)$$

$$\text{s.t. } \mathbf{y} \in Y(\mathbf{x}) \quad (4.14b)$$

$$\left. \begin{aligned} \mathbf{B}(\hat{\mathbf{c}}_l^{(k)} - \boldsymbol{\xi}_l^{(k)}) &\leq \mathbf{b} \\ -\boldsymbol{\eta}_l^{(k)} &\leq \boldsymbol{\xi}_l^{(k)} \leq \boldsymbol{\eta}_l^{(k)} \end{aligned} \right\} \forall k \in K_l \quad (4.14c)$$

$$\left\| \frac{1}{k_l} \sum_{k \in K_l} \boldsymbol{\eta}_l^{(k)} \right\|_p \leq \varepsilon_l. \quad (4.14d)$$

Proof. The result follows by setting $\alpha_l = 0$ and, therefore, optimal $\boldsymbol{\gamma}_l^* = \mathbf{1}$ in the second-level problem reformulation (4.8). \square

We make the following additional assumption:

A6'. For any fixed $\mathbf{x} \in X$, the follower's feasible set is defined as:

$$Y(\mathbf{x}) = \{\mathbf{y} \in \mathbb{R}_+^n : \tilde{\mathbf{F}}\mathbf{y} \leq \tilde{\mathbf{f}}, \mathbf{y} \leq \mathbf{U}(\mathbf{1} - \mathbf{x})\}$$

where $\tilde{\mathbf{F}}$ is unimodular, $\tilde{\mathbf{f}}$ is integral and \mathbf{U} is a diagonal matrix inducing upper bounds on \mathbf{y} .

Although Assumption **A6'** further restricts the class of interdiction problems in [DP], in our pessimistic risk-neutral setting, it is still satisfied by the min-cost flow interdiction problem [46] and the shortest-path interdiction problem [29]. On a positive note, similar to **A6**, Assumption **A6'** allows to treat \mathbf{y} as integer variables and, therefore, simplify the second-level problem in (4.14). The subsequent steps closely follow those for Algorithm 1. Consequently, a detailed discussion of the Benders decomposition algorithm applied to the risk-neutral problem (4.14) is provided in Supplementary Material B (see Algorithm 2).

5. Semi-pessimistic approximation

5.1. Problem formulation and complexity

To address the information gap between the true basic model [DRI*] and its pessimistic approximation [DRI-P], we introduce a *semi-pessimistic approximation* of [DRI*]; recall case (ii) of Example 1. Specifically, we relax Assumption **A3** by introducing the following alternative assumption:

A3'. The leader and the follower have access to two i.i.d. training data sets given by equation (2.4).

Furthermore, for each $k \in K_f$, the leader either knows that

$$\hat{\mathbf{c}}_f^{(k)} \subseteq \hat{S}_l^{(k)} := \left\{ \mathbf{c} \in \mathbb{R}^n : \underline{\mathbf{b}}^{(k)} \leq \mathbf{c} \leq \overline{\mathbf{b}}^{(k)} \right\} \subseteq S$$

or that $\hat{\mathbf{c}}_f^{(k)} \in \hat{\mathbf{C}}_l$.

According to Assumption **A3'**, the leader is aware about a part of the follower's data set $\hat{\mathbf{C}}_f$, whereas the remaining part is known to satisfy some component-wise interval constraints. Formally, based on Assumption **A3'**, we can also define $\hat{S}_l^{(k)} := \{\hat{\mathbf{c}}_f^{(k)}\}$ whenever $\hat{\mathbf{c}}_f^{(k)} \in \hat{\mathbf{C}}_l$ and introduce an uncertainty set

$$\hat{S}_l := \hat{S}_l^{(1)} \times \dots \times \hat{S}_l^{(k_f)} \quad (5.1)$$

that incorporates the leader's initial information about the follower's data.

Taking into account (5.1), the semi-pessimistic approximation of **[DRI*]** reads as:

$$\textbf{[DRI-SP]}: \quad \hat{z}_{sp}^* := \min_{\mathbf{x} \in X} \max_{\hat{\mathbf{C}}_f \in \hat{S}_l} \min_{\mathbf{y}} \left\{ \max_{\mathbb{Q}_l \in \mathcal{Q}_l} \rho_l(\mathbf{y}, \mathbb{Q}_l) \right\} \quad (5.2a)$$

$$\text{s.t. } \mathbf{y} \in \operatorname{argmax}_{\tilde{\mathbf{y}} \in Y(\mathbf{x})} \left\{ \min_{\mathbb{Q}_f \in \mathcal{Q}_f(\hat{\mathbf{C}}_f)} \rho_f(\tilde{\mathbf{y}}, \mathbb{Q}_f) \right\}. \quad (5.2b)$$

That is, the leader in **[DRI-SP]** assumes the worst-case possible realization of the follower's data set with respect to the uncertainty set \hat{S}_l . Similar to the pessimistic approximation **[DRI-P]**, we first establish the computational complexity of **[DRI-SP]**. The following result holds.

Theorem 5. **[DRI-SP]** is Σ_p^2 -hard.

Proof. To establish the result, we use a reduction from the robust optimistic bilevel problem with interval uncertainty [15] given by:

$$\max_{\mathbf{x} \in \tilde{X}} \min_{\mathbf{c}_f \in \tilde{S}} \max_{\mathbf{y}} \mathbf{c}_l^\top \mathbf{y} \quad (5.3a)$$

$$\text{s.t. } \mathbf{y} \in \operatorname{argmax}_{\tilde{\mathbf{y}} \in \tilde{Y}(\mathbf{x})} \mathbf{c}_f^\top \tilde{\mathbf{y}}, \quad (5.3b)$$

where $\tilde{X} = \{0, 1\}^m$,

$$\tilde{Y}(\mathbf{x}) = \{\mathbf{y} \in [0, 1]^n : \tilde{\mathbf{F}}\mathbf{y} + \tilde{\mathbf{L}}\mathbf{x} \leq \tilde{\mathbf{f}}\} \quad \text{and} \quad \tilde{S} = \{\mathbf{c} \in \mathbb{R}^n : -\mathbf{1} \leq \mathbf{c} \leq \mathbf{1}\}.$$

The latter problem is proved to be Σ_p^2 -hard; see Theorem 1 in [15].

To construct an instance of **[DRI-SP]**, we set $X = \tilde{X}$, $Y(\mathbf{x}) = \tilde{Y}(\mathbf{x})$, $S = \hat{S}_l = \tilde{S}$ and assume that both decision-makers are risk-neutral and ambiguity-free, i.e., $\alpha_l = \alpha_f = 0$ and $\varepsilon_l = \varepsilon_f = 0$. In addition, let the leader and the follower each observe unique samples, $\hat{\mathbf{c}}_l := -\mathbf{c}_l \in S$ and $\hat{\mathbf{c}}_f := \mathbf{c}_f \in S$, respectively, with $\hat{\mathbf{c}}_f$ being unknown to the leader.

Given these prerequisites, (5.3) reduces to the following instance of **[DRI-SP]**:

$$- \min_{\mathbf{x} \in X} \max_{\hat{\mathbf{C}}_f \in \hat{S}_l} \min_{\mathbf{y}} \hat{\mathbf{c}}_l^\top \mathbf{y} \quad (5.4a)$$

$$\text{s.t. } \mathbf{y} \in \operatorname{argmax}_{\tilde{\mathbf{y}} \in Y(\mathbf{x})} \hat{\mathbf{c}}_f^\top \tilde{\mathbf{y}}, \quad (5.4b)$$

where we additionally reverse the sign of the leader's objective function. Without loss of generality, we may assume that $\hat{\mathbf{c}}_l \in S = \tilde{S}$, since scaling $\hat{\mathbf{c}}_l$ does not affect the optimal objective function value in (5.4). Hence, (5.3) reduces to an instance of **[DRI-SP]**, and the result follows. \square

5.2. Scenario-based discretization

Since the semi-pessimistic approximation is Σ_2^p -hard, we propose to use a discretization of the uncertainty set (5.1), based on a finite number of scenarios for the follower's data set $\hat{\mathbf{C}}_f$; recall our discussion in Section 1.2. That is, following the sampling-based approach for robust optimization problems proposed by Calafiore and Campi [16, 17], we define a set of $r_l \in \mathbb{N}$ scenarios

$$\hat{S}_l' = \left\{ \hat{\mathbf{C}}_f^{(r)} \in \hat{S}_l, r \in R_l = \{1, \dots, r_l\} \right\}, \quad (5.5)$$

generated from a probability distribution $\mathbb{P} \in \mathcal{Q}_0(\hat{S}_l)$ that is fully supported on \hat{S}_l . Then, instead of directly solving **[DRI-SP]**, we address its *scenario-based discretization* given by:

$$[\mathbf{DRI-SP}'] : \quad \hat{z}_{sp}' = \min_{\mathbf{x} \in X} \max_{\hat{\mathbf{C}}_f \in \hat{S}_l'} \min_{\mathbf{y}} \left\{ \max_{\mathbb{Q}_l \in \mathcal{Q}_l} \rho_l(\mathbf{y}, \mathbb{Q}_l) \right\} \quad (5.6a)$$

$$\text{s.t. } \mathbf{y} \in \operatorname{argmax}_{\tilde{\mathbf{y}} \in Y(\mathbf{x})} \left\{ \min_{\mathbb{Q}_f \in \mathcal{Q}_f(\hat{\mathbf{C}}_f)} \rho_f(\tilde{\mathbf{y}}, \mathbb{Q}_f) \right\}. \quad (5.6b)$$

While the relation between **[DRI-SP']** and **[DRI-SP]** is analyzed in detail later, we first demonstrate that **[DRI-SP']** can be solved by leveraging its single-level MILP formulation.

Theorem 6. *Let Assumptions **A1**, **A2** and **A3'** hold, and the ambiguity sets in (2.5) be defined in terms of p -norm with $p \in \{1, \infty\}$. Then, the discretized semi-pessimistic approximation **[DRI-SP']** admits the following MILP reformulation:*

$$\hat{z}_{sp}' = \min_{\mathbf{x}, \mathbf{y}, \boldsymbol{\nu}, \mathbf{s}, \boldsymbol{\mu}, \boldsymbol{\beta}, \boldsymbol{\gamma}, \boldsymbol{\lambda}, t, z} z \quad (5.7a)$$

$$\text{s.t. } \mathbf{x} \in X \quad (5.7b)$$

$$\left. \begin{aligned} & \hat{\mathbf{c}}_l^{(k)\top} \mathbf{y}^{(r)} - t_l^{(r)} + \boldsymbol{\Delta}_l^{(k)\top} \boldsymbol{\nu}_l^{(k,r)} \leq s_l^{(k,r)} \\ & \|\mathbf{B}^\top \boldsymbol{\nu}_l^{(k,r)} - \mathbf{y}^{(r)}\|_q \leq \lambda_l^{(r)} \\ & \boldsymbol{\nu}_l^{(k,r)} \geq \mathbf{0}, s_l^{(k,r)} \geq 0 \end{aligned} \right\} \forall k \in K_l, \forall r \in R_l \quad (5.7c)$$

$$\left. \begin{aligned} & z \geq t_l^{(r)} + \frac{1}{1-\alpha_l} (\lambda_l^{(r)} \varepsilon_l + \frac{1}{k_l} \sum_{k \in K_l} s_l^{(k,r)}) \\ & (3.4b)-(3.4d), (3.5b)-(3.5f) \\ & (\mathbf{f} - \mathbf{L}\mathbf{x})^\top \boldsymbol{\beta}_f^{(r)} = t_f^{(r)} - \frac{1}{1-\alpha_f} (\varepsilon_f \lambda_f^{(r)} + \frac{1}{k_f} \sum_{k \in K_f} s_f^{(k,r)}) \end{aligned} \right\} \forall r \in R_l, \quad (5.7d)$$

where $\boldsymbol{\Delta}_l^{(k)} = \mathbf{b} - \mathbf{B}\hat{\mathbf{c}}_l^{(k)} \geq \mathbf{0}$ for each $k \in K_l$ and $\frac{1}{p} + \frac{1}{q} = 1$.

Proof. See Supplementary Material A. □

Thus, in line with the results of Buchheim et al. [15], discretization allows to reduce the computational complexity of **[DRI-SP]**. Nevertheless, **[DRI-SP']** is an outer approximation of **[DRI-SP]** and, hence, for a fixed number of scenarios r_l , it may lead to overly optimistic estimates of the true follower's data set $\hat{\mathbf{C}}_f^*$. In other words, it is possible for the optimal objective function value of **[DRI*]** to exceed that of **[DRI-SP']**, i.e., $z_b^* > \hat{z}_{sp}'$.

Notably, under mild assumptions, Calafiore and Campi [16, 17] establish probabilistic guarantees on the number of scenarios required to discretize convex optimization problems under uncertainty. However, the approach in [16, 17] is not applicable to **[DRI-SP]**, as the feasible set X is discrete and, moreover, the objective function in **[DRI-SP]** is not convex in \mathbf{x} for a fixed realization of uncertainty $\hat{\mathbf{C}}_f \in \hat{S}_l$. We illustrate this non-convexity with the following example.

Example 2. Consider the instance of **[DRI-SP]** used in the proof of Theorem 6; see equation (5.4). Then, for a given $\hat{\mathbf{c}}_f \in \hat{S}_l$, let

$$\begin{aligned} \varphi(\mathbf{x}) &:= \min_{\mathbf{y}} \hat{\mathbf{c}}_l^\top \mathbf{y} \\ \text{s.t. } \mathbf{y} &\in \operatorname{argmax}_{\tilde{\mathbf{y}} \in Y(\mathbf{x})} \hat{\mathbf{c}}_f^\top \tilde{\mathbf{y}}. \end{aligned}$$

Additionally, let $\hat{\mathbf{c}}_l = (-1, 1)^\top$, $\hat{\mathbf{c}}_f = (1, 1)^\top$ and

$$Y(\mathbf{x}) = \{\mathbf{y} \in [0, 1]^2 : y_1 + y_2 \leq 1, \quad y_i \leq 1 - x_i \quad \forall i \in \{1, 2\}\}.$$

We observe that $\varphi(0, 0) = -1$, $\varphi(1, 1) = 0$ and $\varphi(\frac{1}{2}, \frac{1}{2}) = 0$. Therefore,

$$\varphi(\frac{1}{2}, \frac{1}{2}) = 0 > \frac{1}{2}\varphi(0, 0) + \frac{1}{2}\varphi(1, 1) = -\frac{1}{2}$$

and the function $\varphi(\mathbf{x})$ is not convex in \mathbf{x} . □

On a positive note, even in the absence of convexity, we establish that our discretization **[DRI-SP']** is *asymptotically robust* with respect to the true basic model **[DRI*]**. In other words, it is proved that, as the number of scenarios, r_l , approaches infinity, the inequality $\hat{z}'_{sp} \geq z_b^*$ holds with probability one.

Theorem 7. *Let Assumptions A1, A2 and A3' hold. Also, let \hat{z}'_{sp} and z_b^* denote the optimal objective function values of **[DRI-SP']** and **[DRI*]**, respectively. Then, as r_l tends to infinity, for any scenario-generating distribution $\mathbb{P} \in \mathcal{Q}_0(\hat{S}_l)$ and $\delta' > 0$, the inequality*

$$\hat{z}'_{sp} \geq z_b^* - \delta' \tag{5.8}$$

holds almost surely.

Proof. We define the optimal objective function values of **[DRI-SP']** and **[DRI*]**, respectively, as:

$$\begin{aligned} \hat{z}'_{sp}(r_l) &= \min_{\mathbf{x} \in X} \max_{\hat{\mathbf{C}}_f \in \hat{S}'_l} \min_{\mathbf{y}} \left\{ \max_{\mathbb{Q}_l \in \mathcal{Q}_l} \rho_l(\mathbf{y}, \mathbb{Q}_l) : \mathbf{y} \in \hat{V}_f(\mathbf{x}, \hat{\mathbf{C}}_f) \right\} \quad \text{and} \\ z_b^* &= \min_{\mathbf{x} \in X} \min_{\mathbf{y}} \left\{ \max_{\mathbb{Q}_l \in \mathcal{Q}_l} \rho_l(\mathbf{y}, \mathbb{Q}_l) : \mathbf{y} \in \hat{V}_f(\mathbf{x}, \hat{\mathbf{C}}_f^*) \right\}, \end{aligned}$$

where

$$\hat{V}_f(\mathbf{x}, \hat{\mathbf{C}}_f) = \operatorname{argmax}_{\tilde{\mathbf{y}} \in Y(\mathbf{x})} \left\{ \min_{\mathbb{Q}_f \in \mathcal{Q}_f(\hat{\mathbf{C}}_f)} \rho_f(\tilde{\mathbf{y}}, \mathbb{Q}_f) \right\}.$$

First, by passing to a subsequence if necessary, we note that almost surely

$$\lim_{r_l \rightarrow \infty} \hat{\mathbf{C}}_f^{(r_l)} = \hat{\mathbf{C}}_f^*, \quad (5.9)$$

where the convergence is understood componentwise. Indeed, for any distribution $\mathbb{P} \in \mathcal{Q}_0(\hat{S}_l)$ fully supported on \hat{S}_l , let $\{\hat{\mathbf{C}}_f^{(r)}\}_{r \in R_l}$ be an i.i.d. sample sequence generated from \mathbb{P} . Then, as r_l tends to infinity, the second Borel-Cantelli lemma implies that infinitely many samples fall arbitrarily close to any $\hat{\mathbf{C}}_f^* \in \hat{S}_l$ almost surely and, hence, (5.9) holds.

Next, we prove that inequality (5.8) holds with probability 1, given that $r_l \rightarrow \infty$, i.e.,

$$\lim_{r_l \rightarrow \infty} \Pr \left\{ \hat{z}_{sp}^*(r_l) \geq z_b^* - \delta' \right\} = 1. \quad (5.10)$$

Assume, to the contrary, that there exist $\eta > 0$ and $\bar{r} \in \mathbb{N}$, such that for all $r_l \geq \bar{r}$

$$\Pr \left\{ \hat{z}_{sp}^*(r_l) < z_b^* - \delta' \right\} = 1 - \Pr \left\{ \hat{z}_{sp}^*(r_l) \geq z_b^* - \delta' \right\} \geq \eta > 0.$$

To establish the contradiction, we analyze the inequality

$$\hat{z}_{sp}^*(r_l) < z_b^* - \delta' \quad (5.11)$$

for sufficiently large r_l . Thus, (5.11) implies that there exists $\mathbf{x}' \in X$ such that:

$$\max_{\hat{\mathbf{C}}_f \in \hat{S}'_l} \min_{\mathbf{y}} \left\{ \max_{\mathbb{Q}_l \in \mathcal{Q}_l} \rho_l(\mathbf{y}, \mathbb{Q}_l) : \mathbf{y} \in \hat{V}_f(\mathbf{x}', \hat{\mathbf{C}}_f) \right\} < \min_{\mathbf{y}} \left\{ \max_{\mathbb{Q}_l \in \mathcal{Q}_l} \rho_l(\mathbf{y}, \mathbb{Q}_l) : \mathbf{y} \in \hat{V}_f(\mathbf{x}', \hat{\mathbf{C}}_f^*) \right\} - \delta'$$

and, therefore, for each $r \leq r_l$, we have:

$$\min_{\mathbf{y}} \left\{ \max_{\mathbb{Q}_l \in \mathcal{Q}_l} \rho_l(\mathbf{y}, \mathbb{Q}_l) : \mathbf{y} \in \hat{V}_f(\mathbf{x}', \hat{\mathbf{C}}_f^{(r)}) \right\} < \min_{\mathbf{y}} \left\{ \max_{\mathbb{Q}_l \in \mathcal{Q}_l} \rho_l(\mathbf{y}, \mathbb{Q}_l) : \mathbf{y} \in \hat{V}_f(\mathbf{x}', \hat{\mathbf{C}}_f^*) \right\} - \delta'. \quad (5.12)$$

Next, by Lemma 3, the follower's set of optimal solutions $\hat{V}_f(\mathbf{x}', \hat{\mathbf{C}}_f)$ is non-empty and upper semicontinuous. Therefore, by passing to a subsequence if necessary, we have:

$$\limsup_{r_l \rightarrow \infty} \hat{V}_f(\mathbf{x}', \hat{\mathbf{C}}_f^{(r_l)}) \subseteq \hat{V}_f(\mathbf{x}', \hat{\mathbf{C}}_f^*). \quad (5.13)$$

Finally, we show that the relation in (5.13) forces the inequality in (5.12) to be violated. Indeed, by applying similar reasoning as in the proof of Lemma 3, one may observe that the leader's objective function

$$v_l(\mathbf{y}) := \max_{\mathbb{Q}_l \in \mathcal{Q}_l} \rho_l(\mathbf{y}, \mathbb{Q}_l)$$

is continuous in \mathbf{y} . Moreover, (5.12) for $r = r_l$ can be expressed as:

$$v_l(\mathbf{y}^{*(r_l)}) < v_l(\mathbf{y}^*) - \delta', \quad (5.14)$$

where $\mathbf{y}^{*(r_l)}$ and \mathbf{y}^* are optimal solutions, respectively, for the left- and the right-hand side of (5.12). The upper semicontinuity (5.13) implies that we can always select

$$\lim_{r_l \rightarrow \infty} \mathbf{y}^{*(r_l)} = \tilde{\mathbf{y}}^* \in \hat{V}_f(\mathbf{x}', \hat{\mathbf{C}}_f^*)$$

as an accumulation point of $\mathbf{y}^{*(r_l)}$, $r_l \in \{1, \dots, \infty\}$. Then, since $v_l(\mathbf{y}^*) \leq v_l(\tilde{\mathbf{y}}^*)$, the contradiction is obtained by taking the limit in (5.14) with respect to r_l . As a result, we have

$$\lim_{r_l \rightarrow \infty} \Pr \left\{ \hat{z}_{sp}^*(r_l) < z_b^* - \delta' \right\} = 0.$$

Hence, (5.10) holds, and the result follows. \square

Importantly, Theorem 6 does not exploit discreteness of the leader's feasible set X and, hence, it also applies to mixed-integer or convex feasible sets. As a potential drawback, we note that the proposed discretization of the semi-pessimistic approximation $[\mathbf{DRI-SP}']$ is still a *heuristic* that enjoys only asymptotic performance guarantees. At the same time, in practice, we show that inequality (5.8) may also hold with a sufficiently small number of scenarios, r_l , even for relatively large uncertainty sets $\hat{S}_l^{(k)}$, $k \in K_f$; see Section 6.

6. Computational study

Building upon Example 1, our computational study examines the basic model $[\mathbf{DRI}]$, along with the scenario-based semi-pessimistic and pessimistic approximations, $[\mathbf{DRI-SP}']$ and $[\mathbf{DRI-P}]$. All models are evaluated using synthetic test instances from the packing interdiction problem [24]; see Section 6.1. In Section 6.2, we analyze the out-of-sample errors, arising from the leader's and the follower's limited knowledge of the true distribution \mathbb{Q}^* within the basic model $[\mathbf{DRI}]$. It is also explored how the decision-makers' risk preferences influence the model's out-of-sample performance. Next, in Section 6.3, by leveraging approximations $[\mathbf{DRI-SP}']$ and $[\mathbf{DRI-P}]$ of the true basic model $[\mathbf{DRI}^*]$, we assess both in-sample and out-of-sample errors of the leader due to its incorrect perception of the true follower's policy. Finally, a brief analysis of running times for all the aforementioned models is provided; see Section 6.4.

6.1. Test instances and performance measures

Test instances. Similar to Zare et al. [52], we consider a class of general interdiction problems defined as:

$$\min_{\mathbf{x} \in X} \max_{\mathbf{y} \in Y(\mathbf{x})} \mathbf{c}^\top \mathbf{y}, \quad (6.1)$$

where

$$X = \{ \mathbf{x} \in \{0, 1\}^n : \mathbf{H}\mathbf{x} \leq \mathbf{h} \} \quad \text{and} \quad Y(\mathbf{x}) = \{ \mathbf{y} \in \mathbb{R}_+^n : \tilde{\mathbf{F}}\mathbf{y} \leq \tilde{\mathbf{f}}, \mathbf{y} \leq \mathbf{U}(1 - \mathbf{x}) \}. \quad (6.2)$$

In our experiments, we fix $d_l = \dim(\mathbf{h}) = 1$ and $\tilde{d}_f = \dim(\tilde{\mathbf{f}}) = 10$. Furthermore, all elements of \mathbf{H} and $\tilde{\mathbf{F}}$ in (6.2) are generated uniformly at random from the interval $[0.01, 1]$, whereas

$$h_j = 0.4 \sum_{i=1}^n H_{ji} \quad \forall j \in \{1, \dots, d_l\}, \quad f_j = 0.4 \sum_{i=1}^n F_{ji} \quad \forall j \in \{1, \dots, \tilde{d}_f\}$$

and $\mathbf{U} = \mathbf{I}$. Given that the profit vector \mathbf{c} is also nonnegative, (6.1) can be viewed as an instance of the packing interdiction problem [24]. In particular, it can be verified that $Y(\mathbf{x})$ is non-empty and bounded for every fixed $\mathbf{x} \in X$, which aligns with Assumption **A1**.

With respect to the profit vector \mathbf{c} , we introduce an interval support set given by:

$$S := \{\mathbf{c} \in \mathbb{R}^n : c_i \in [0.01, 1] \quad \forall i \in N := \{1, \dots, n\}\}. \quad (6.3)$$

Then, the true distribution \mathbb{Q}^* is defined as a product of marginal distributions for each component c_i , $i \in N$. Specifically, we assume that c_i is governed by a *truncated normal distribution*, constructed as follows. First, we draw samples from a normal distribution with mean $\mu_i = \frac{0.5i}{n+1}$ and standard deviation

$$\sigma_i = 0.05 + \frac{0.04i}{n+1} \quad \forall i \in N. \quad (6.4)$$

These samples are then truncated to the interval $[0, 1]$ and subsequently scaled to the range $[0.01, 1]$. Our data-generating distribution is somewhat similar to the return distribution considered by Esfahani and Kuhn [25] in the context of a portfolio optimization problem, where larger returns are associated with higher risk. At the same time, in line with Assumption **A2**, the support set (6.3) is compact. To facilitate qualitative analysis, we set $n = 10$ and generate 10 *fixed* random test instances of the packing interdiction problem (6.1). Each instance is then evaluated across 10 independently generated data sets sampled from \mathbb{Q}^* .

Finally, the core parameters of our basic model [**DRI**] are defined as follows. By default, $\alpha_l = 0.95$ and $\alpha_f = 0.95$ represent risk-averse scenarios for the leader and the follower, respectively; risk-neutral scenarios are attained by setting $\alpha_l = 0$ and $\alpha_f = 0$. Next, we note that, in many practical applications, the Wasserstein radius can be tuned via cross-validation to achieve optimal out-of-sample performance; see, e.g., [25]. However, the Wasserstein radii ε_l and ε_f in [**DRI**] are inherently dependent, with the optimal choice of ε_f potentially depending on the leader's decision $\mathbf{x} \in X$. For this reason, we prefer to use the following analytical expressions for these parameters:

$$\varepsilon_l := \frac{\delta_l}{\sqrt{k_l}} \quad \text{and} \quad \varepsilon_f := \frac{\delta_f}{\sqrt{k_f}}, \quad (6.5)$$

where $\delta_l \in \mathbb{Z}_+$ and $\delta_f \in \mathbb{Z}_+$ are appropriate constants that may depend on the problem's dimension. This approach leverages the convergence rate proportional to $k_l^{-\frac{1}{2}}$ (or, respectively, $k_f^{-\frac{1}{2}}$), which is considered theoretically optimal and achievable in practice; see, e.g., [25, 36]. Also, by setting $p = 1$, we consider the Wasserstein distance with respect to ℓ_1 -norm.

To generate scenarios for the scenario-based approximation [**DRI-SP'**], we define the uncertainty

set \hat{S}_l given by equation (5.1). Thus, it is assumed that the first $k_{lf} \leq k_f$ samples in the true follower's data set $\hat{\mathbf{C}}_f^*$ are known to the leader. In contrast, for each $k \in \{k_{lf} + 1, \dots, k_f\}$ and $i \in N$, let

$$(\hat{\mathbf{c}}_f^{(k)})_i \in [c_{ki}^* - \kappa \Delta_{ki}, c_{ki}^* + \kappa(1 - \Delta_{ki})] \cap [0.01, 1].$$

Here, c_{ki}^* is the nominal value used by the follower, κ represents a fixed noise level, and $\Delta_{ki} \in [0, 1]$ is a shift parameter. For each of the 10 test instances, Δ_{ki} is defined as follows: it is set to 0 with probability 0.5, and with the remaining probability 0.5, it is selected uniformly at random from the interval $[0, 1]$. In other words, approximately 50% of the data entries in the remaining $k_f - k_{lf}$ samples are subject to interval uncertainty. Following [16, 17], the sample-generating distribution \mathbb{P} is supposed to be uniform on \hat{S}_l .

For the sake of comparison, we also consider the *augmented basic model*; recall case (iii) of Example 1. For simplicity, within the comparison we always assume that $k_l = k_f$ and, consequently, the augmented basic model reduces to the basic model [DRI], with the follower's data set replaced by the leader's data set. With a slight abuse of notation, this model is also referred to as [DRI].

Computational settings. All experiments are performed on a PC with CPU i9-12900U and RAM 32 GB. The MILP reformulations (3.6) and (5.7), as well as the Benders decomposition algorithms (Algorithm 1 and Algorithm 2), are implemented in Java using CPLEX 22.1. We set the tolerance level $\delta = 10^{-3}$ for both Algorithms 1 and 2. We also discuss our approach to linearization of (3.6) and other related MILP reformulations in Supplementary Material B. The respective code can be found at <https://github.com/sk19941995/Data-driven-interdiction>.

Performance measures. First, we define *relative out-of-sample loss* of the leader and the follower in the basic model [DRI]. Let $(\hat{\mathbf{x}}^*, \hat{\mathbf{y}}^*)$ be an optimal solution of the MILP reformulation (3.6). Then, the relative out-of-sample loss of the follower is defined as:

$$\text{RL}_f^{(out)}(\hat{\mathbf{x}}^*, \hat{\mathbf{y}}^*, \mathbb{Q}^*) = \frac{\rho_f(\hat{\mathbf{y}}^*, \mathbb{Q}^*)}{\max_{\mathbf{y} \in Y(\hat{\mathbf{x}}^*)} \rho_f(\mathbf{y}, \mathbb{Q}^*)}. \quad (6.6)$$

It follows that $\text{RL}_f^{(out)} \leq 1$ and $\text{RL}_f^{(out)} = 1$ if and only if $\hat{\mathbf{y}}^*$ is an optimal solution of the full-information follower's problem with $\mathbf{x} = \hat{\mathbf{x}}^*$. In a similar way, the leader's relative out-of-sample loss is defined as:

$$\text{RL}_l^{(out)}(\hat{\mathbf{x}}^*, \hat{\mathbf{y}}^*, \mathbb{Q}^*) = \frac{\rho_l(\hat{\mathbf{y}}^*, \mathbb{Q}^*)}{\rho_l(\tilde{\mathbf{y}}^*, \mathbb{Q}^*)}, \quad (6.7)$$

where $\tilde{\mathbf{y}}^*$ solves the following full information leader's problem:

$$\min_{\mathbf{x}, \mathbf{y}} \rho_l(\mathbf{y}, \mathbb{Q}^*) \quad (6.8a)$$

$$\text{s.t. } \mathbf{x} \in X \quad (6.8b)$$

$$\mathbf{y} \in \arg\max_{\tilde{\mathbf{y}} \in Y(\mathbf{x})} \left\{ \min_{\mathbb{Q}_f \in \mathcal{Q}_f(\hat{\mathbf{C}}_f^*)} \rho_f(\tilde{\mathbf{y}}, \mathbb{Q}_f) \right\}. \quad (6.8c)$$

In other words, (6.8) is the true basic model [DRI*], where the leader also has full information about the true distribution \mathbb{Q}^* . Since $(\hat{\mathbf{x}}^*, \hat{\mathbf{y}}^*)$ is also feasible in (6.8), we have $\text{RL}_l^{(out)} \geq 1$ and $\text{RL}_l^{(out)} = 1$ if

and only if $(\hat{\mathbf{x}}^*, \hat{\mathbf{y}}^*)$ is an optimal solution of the full information problem (6.8). It is worth mentioning that instead of computing the ratios in (6.6) and (6.7) explicitly, we use a sample average approximation based on 1000 samples generated from \mathbb{Q}^* .

Next, for **[DRI-SP']** and **[DRI-P]**, the relative out-of-sample loss of the leader is defined as follows. Given that $\hat{\mathbf{x}}^* \in X$ is the associated optimal leader's decision, we introduce

$$\text{RL}_l^{(out)}(\hat{\mathbf{x}}^*, \mathbb{Q}^*) = \frac{\rho_l(\hat{\mathbf{y}}^*, \mathbb{Q}^*)}{\rho_l(\tilde{\mathbf{y}}^*, \mathbb{Q}^*)}, \quad (6.9)$$

where $\tilde{\mathbf{y}}^*$ is an optimal solution of (6.8) and $\hat{\mathbf{y}}^*$ is an optimal solution of (6.8) with an additional constraint $\mathbf{x} = \hat{\mathbf{x}}^*$. Finally, the *relative in-sample loss* for any approximation of the true basic model **[DRI*]** is defined as:

$$\text{RL}_l^{(in)} = \frac{\hat{z}^*}{z_b^*}. \quad (6.10)$$

Here, z_b^* is the optimal objective function value of the true basic model **[DRI*]**, whereas \hat{z}^* is the optimal objective function value of its approximation, **[DRI-SP']** or **[DRI-P]**. The in-sample and the out-of-sample relative losses for the augmented basic model **[DRI]** are defined precisely in the same way as for the aforementioned approximations.

6.2. Analysis of basic model

In the first set of experiments, the leader's and the follower's out-of-sample performance are analyzed within the basic model **[DRI]**. Due to Assumption **A3**, we set $k_f \leq k_l$ and generate the follower's data set $\hat{\mathbf{C}}_f$ as a part of the leader's data set $\hat{\mathbf{C}}_l$.

Initially, we set $k_l = k_f = 30$ and examine the follower's relative loss (6.6) and the leader's relative loss (6.7) as functions of δ_f and δ_l , respectively; recall equation (6.5). Thus, Figures 1a and 1b present the average relative loss of the follower and the leader, respectively, along with mean absolute deviations (MADs), computed over 100 random test instances; recall that we generate 10 random test instances of the packing interdiction problem (6.1), with 10 different data sets for each instance.

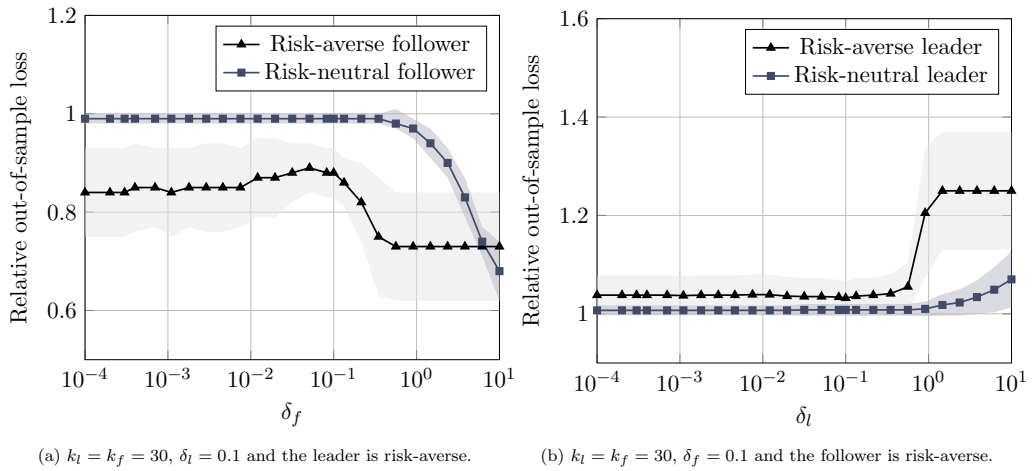


Figure 1: The average relative out-of-sample loss (with MADs) of the follower (6.6) (a) and the leader (6.7) (b) as a function of δ_f and δ_l , respectively, evaluated over 100 random test instances.

We make the following observations:

- Similar to the one-stage DRO model in [25], for both the risk-averse leader and the risk-averse follower, the relative out-of sample loss first tends to improve and then deteriorates with the increase of the Wasserstein radius. In other words, both decision-makers alternate between the sample average ($\varepsilon_l = 0$ or $\varepsilon_f = 0$) and the robust regimes ($\varepsilon_l = \infty$ or $\varepsilon_f = \infty$), with a potential improvement in-between these two regimes.
- For both the risk-averse leader and the risk-averse follower, a *critical radius* can be identified at approximately $\varepsilon_l \approx \frac{0.1}{\sqrt{30}}$ and $\varepsilon_f \approx \frac{0.1}{\sqrt{30}}$, corresponding to the best achievable out-of-sample performance. Meanwhile, the DRO approach yields a relative gain of about 5% over the sample average approximation (SAA) for the risk-averse follower, but only about 1% for the risk-averse leader. One possible explanation for this observation is that the leader’s decision variables are binary, while the follower’s decision variables are continuous.
- On the other hand, neither the risk-neutral leader nor the risk-neutral follower achieves any relative gain. This outcome is somewhat expected, given our choice of the ℓ_1 -norm; see, e.g., Lemma 2 in [34].
- Finally, we observe that the robust regime for the risk-averse decision-makers is achieved at smaller values of δ_l and δ_f compared to the risk-neutral decision-makers. In this regard, we note that the conditional value-at-risk can be viewed as an additional layer of robustness with respect to the risk-neutral objective function.

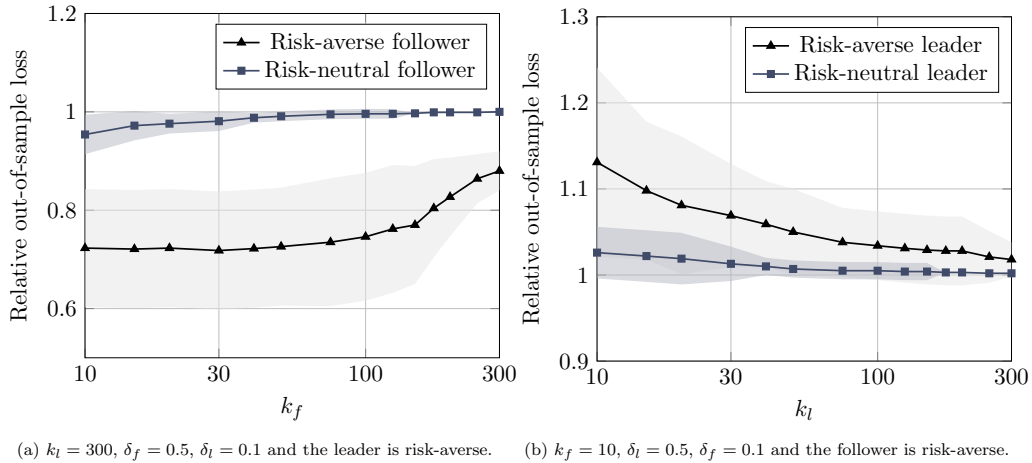


Figure 2: The average relative out-of-sample loss (with MADs) of the follower (6.6) (a) and the leader (6.7) (b) as a function of their respective sample sizes, evaluated over 100 random test instances.

Next, we use the relative out-of-sample losses (6.6) and (6.7) to analyze convergence, respectively, for the leader and the follower; see Figures 2a and 2b. We make the following observations:

- As suggested by Lemma 2, the follower’s relative loss in (6.6) almost surely converges to 1 as k_f tends to infinity, irrespective of the leader’s decision $\mathbf{x} \in X$.
- As suggested by Theorem 2, the leader’s relative loss in (6.7) almost surely converges to 1 as k_l approaches infinity, even when k_f remains fixed; see equation (3.17).

- Based on Figures 2a and 2b, we conclude that the convergence is faster for the case of the risk-neutral decision-makers. This observation is rather natural, given that the selected parameters $\delta_f = 0.5$ and $\delta_l = 0.5$ correspond to different regimes for the risk-averse and the risk-neutral decision-makers; recall Figures 1a and 1b.

Finally, we conduct a detailed analysis of the decision-makers' risk preferences by examining different combinations of risk-neutral (N) and risk-averse (A) regimes for both the leader and the follower. For each combination of regimes and the associated optimal solution $(\hat{\mathbf{x}}^*, \hat{\mathbf{y}}^*)$ of the MILP reformulation (3.6), we compute the true right-tail and the true left-tail CVaRs, $\rho_l(\hat{\mathbf{y}}^*, \mathbb{Q}^*)$ and $\rho_f(\hat{\mathbf{y}}^*, \mathbb{Q}^*)$, as well as the true mean, which is obtained by setting $\alpha_l = 0$ or $\alpha_f = 0$; see Table 3.

Sample sizes	Risk preferences	True risk measure		
		Left-tail CVaR	Mean	Right-tail CVaR
$k_l = k_f = 30$	NN	0.37 (0.05)	0.95 (0.09)	1.62 (0.14)
	NA	0.37 (0.03)	0.76 (0.05)	1.21 (0.08)
	AN	0.38 (0.05)	0.96 (0.09)	1.63 (0.14)
	AA	0.39 (0.03)	0.78 (0.06)	1.22 (0.08)
$k_l = k_f = 300$	NN	0.36 (0.04)	0.94 (0.09)	1.60 (0.15)
	NA	0.39 (0.04)	0.81 (0.07)	1.29 (0.10)
	AN	0.38 (0.05)	0.94 (0.10)	1.60 (0.14)
	AA	0.40 (0.05)	0.82 (0.07)	1.28 (0.10)

(a)

Sample sizes	Risk preferences	True risk measure		
		Left-tail CVaR	Mean	Right-tail CVaR
$k_l = k_f = 30$	NN	0.50 (0.09)	0.98 (0.07)	1.56 (0.10)
	NA	0.50 (0.07)	0.90 (0.06)	1.38 (0.08)
	AN	0.67 (0.13)	1.06 (0.10)	1.53 (0.11)
	AA	0.60 (0.09)	0.95 (0.07)	1.36 (0.08)
$k_l = k_f = 300$	NN	0.50 (0.08)	0.98 (0.07)	1.57 (0.08)
	NA	0.52 (0.08)	0.93 (0.07)	1.41 (0.09)
	AN	0.67 (0.12)	1.05 (0.08)	1.48 (0.09)
	AA	0.72 (0.13)	1.01 (0.09)	1.32 (0.07)

(b)

Table 3: The average out-of-sample performance (with MADs) of the decision-makers with varying risk preferences, for $\delta_l = \delta_f = 0.1$, evaluated over 100 random test instances. The true data-generating distribution has variances either proportional (a) or *inversely* proportional (b) to the mean. Symbols “N” and “A” in column 2 represent risk-neutral and risk-averse policies, respectively, while the first letter refers to the leader’s policy and the second letter refers to the follower’s policy. The policy that is beneficial for both the leader and the follower is highlighted in bold.

In this experiment, we consider two classes of data-generating distributions, where σ_i , $i \in N$, is either proportional to the mean, as defined by equation (6.4), or inversely proportional to the mean, i.e.,

$$\sigma_i = 0.05 + \left(0.04 - \frac{0.04i}{n+1}\right) \quad \forall i \in N;$$

see Tables 3a and 3b, respectively. The second class of distributions serves to clearly illustrate the contrast between the risk-neutral and the risk-averse regimes for the leader; see, e.g., the values in rows NN and AN. More specifically, when the variance is proportional to the mean, the leader’s optimal solution in the risk-averse case (A) often coincides with the one in the risk-neutral case (N), leading to similar out-of-sample performance. For both distribution classes, we identify policy combinations that are *mutually beneficial* for the leader and the follower; in Table 3, these combinations are highlighted in bold. Furthermore, given that the risk-averse regime is shown to exhibit slower convergence, we analyze both small ($k_l = k_f = 30$) and large ($k_l = k_f = 300$) sample sizes.

We observe that, for small sample sizes, the risk-neutral policy is generally beneficial for both decision-makers. However, for large sample sizes, the neutral-averse (NA) and the averse-neutral (AN) policies become beneficial under the left and the right-tail CVaRs, respectively. This trend can be explained by the fact that these policies are, in a sense, the “closest” approximations of the respective true risk measures. What is even more interesting is that the averse-averse (AA) policy, while theoretically justified, is generally not beneficial. Specifically, for large sample sizes, it is only preferable for the follower under the left-tail CVaR, and only for the leader under the right-tail CVaR. Therefore, adopting the AA policy makes sense only if avoiding both extremely small and large profits is deemed more important than optimizing average gains.

6.3. Analysis of semi-pessimistic and pessimistic approximations

We begin with analyzing the scenario-based semi-pessimistic approximation **[DRI-SP']** in terms of the leader’s relative out-of-sample and in-sample losses, (6.9) and (6.10), as a function of the number of scenarios, $r_l \in \{1, \dots, 10\}$; see Figure 3. In particular, we set $k_{lf} = 20$ and $k_f = 30$, i.e., one-third of the follower’s data set is subject to uncertainty, and examine medium and large noise levels, $\kappa = 0.2$ and $\kappa = 0.5$. To verify robustness of **[DRI-SP']**, in addition to the average in-sample relative loss, for each r_l , we provide its empirical 5% percentile. For the sake of comparison, we also indicate the results for the underlying augmented basic model **[DRI]** and the true basic model **[DRI*]** that are not affected by the number of scenarios.

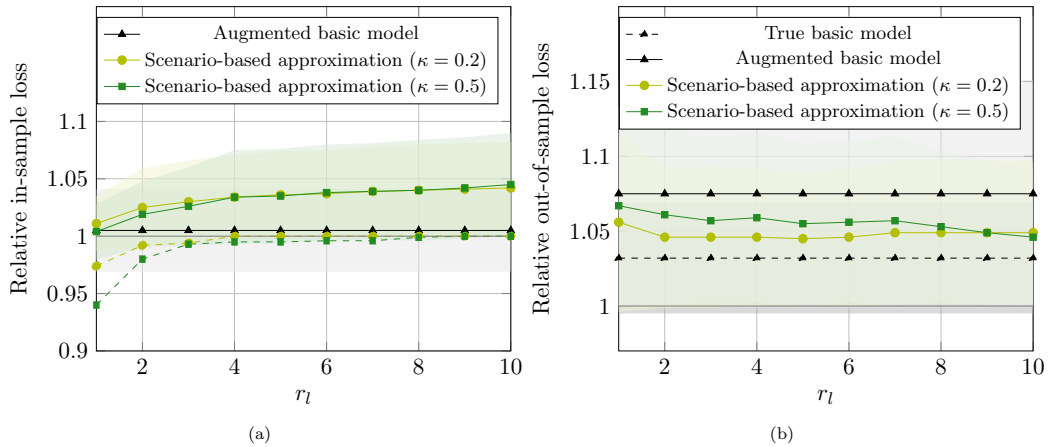


Figure 3: The average relative in-sample (6.9) (a) and out-of-sample (6.10) (b) loss (with MADs) as a function of the number of scenarios, r_l , for $k_l = k_f = 30$, $\delta_l = \delta_f = 0.1$ and $k_{lf} = 20$, evaluated over 100 random test instances. The dashed lines in (a) correspond to the empirical 5% percentile of the relative in-sample loss.

Based on Figure 3, we make the following observations:

- As suggested by Theorem 7, **[DRI-SP']** tends to become more robust in relation to **[DRI*]**, with the increase of the number of scenarios, r_l ; see Figure 3a. While robustness is achieved on average, i.e., the average relative in-sample loss is larger than 1, about 5% of the test instances for $r_l = 10$ may violate robustness.
- With the increase of the noise level κ , the average in-sample loss tends to increase faster as a function of r_l , providing however a worse 5% percentile. Indeed, larger uncertainty sets cause

greater variability in the follower’s data, leading to less stable results with a small number of scenarios and more conservative results as r_l increases.

- With respect to the out-of-sample performance of $[\mathbf{DRI}\text{-}\mathbf{SP}']$, it first tends to improve and then does not change significantly, as a function of r_l . Overall, the additional out-of-sample error of $[\mathbf{DRI}\text{-}\mathbf{SP}']$ in relation to $[\mathbf{DRI}^*]$ is quite small and uniformly bounded by 3–4% on average.
- The augmented basic model $[\mathbf{DRI}]$ shows no significant relationship with the true model $[\mathbf{DRI}^*]$, resulting in overly optimistic in-sample and relatively poor out-of-sample performance.

Notably, for larger-scale problems, increasing the number of scenarios significantly raises the computational complexity of the MILP reformulation (5.7). While this may also enhance robustness, as illustrated in Figure 3a, we believe that, after some point, the marginal benefit of additional scenarios may not translate into substantial gains in the leader’s out-of-sample performance. For example, based on Figure 3a, we fix $r_l = 5$ in the remainder of the analysis.

In the following, we compare $[\mathbf{DRI}\text{-}\mathbf{SP}']$ with the pessimistic approximation $[\mathbf{DRI}\text{-}\mathbf{P}]$ and the augmented basic model $[\mathbf{DRI}]$ for the ambiguity-free leader ($\varepsilon_l = 0$); see Figure 4. Specifically, the common number of samples, k_{lf} , is increased from 0 to 30, with the true follower’s data set being fixed and $k_l = k_f = 30$. Finally, we set $\alpha_l = 0.9$ to satisfy Assumption A6.

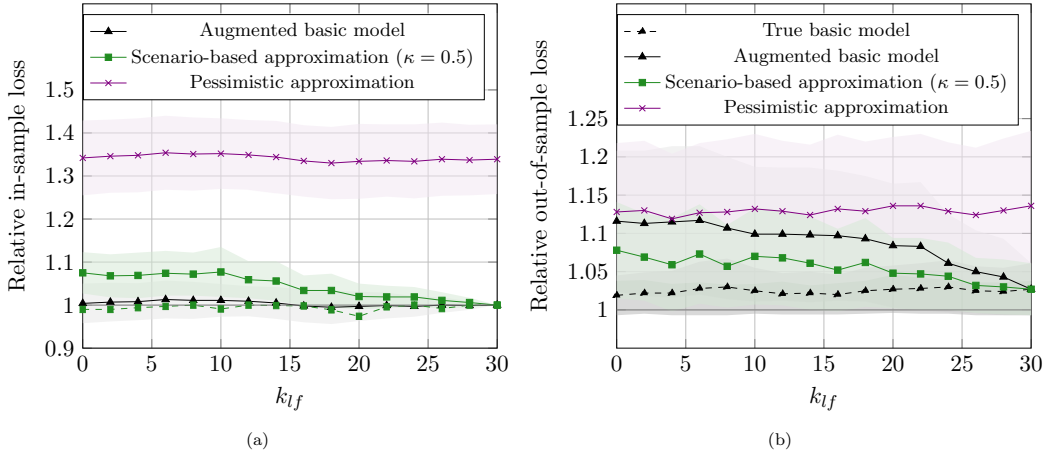


Figure 4: The average relative in-sample (6.9) (a) and out-of-sample (6.10) (b) loss of the *ambiguity-free* leader (with MADs) as a function of the common sample size, k_{lf} , for $k_l = k_f = 30$, $\delta_l = \delta_f = 0.1$ and $\alpha_l = 0.9$, evaluated over 100 random test instances. The follower is assumed to be risk-averse. The dashed line corresponds to the empirical 5% percentile of the relative in-sample loss for the scenario-based semi-pessimistic approximation.

From Figure 4, we observe that the relative in-sample loss of the leader in $[\mathbf{DRI}\text{-}\mathbf{SP}']$ and $[\mathbf{DRI}]$ converges to 1 as the leader acquires more data from the follower. A similar trend is observed in terms of the relative out-of-sample performance, i.e., both models converge to the true basic model $[\mathbf{DRI}^*]$. Importantly, both $[\mathbf{DRI}]$ and $[\mathbf{DRI}\text{-}\mathbf{P}]$ exhibit poor out-of-sample performance. Even when the leader is entirely uncertain about the follower’s data ($k_{lf} = 0$), meaning that approximately half of all data entries are subject to severe noise ($\kappa = 0.5$), the scenario-based approximation $[\mathbf{DRI}\text{-}\mathbf{SP}']$ still significantly outperforms both outlined models. It can be explained by the fact that the augmented basic model $[\mathbf{DRI}]$ substantially alters the follower’s data set. At the same time, the pessimistic approximation $[\mathbf{DRI}\text{-}\mathbf{P}]$ not only disregards the follower’s data but also overlooks the structure of the

follower's objective function.

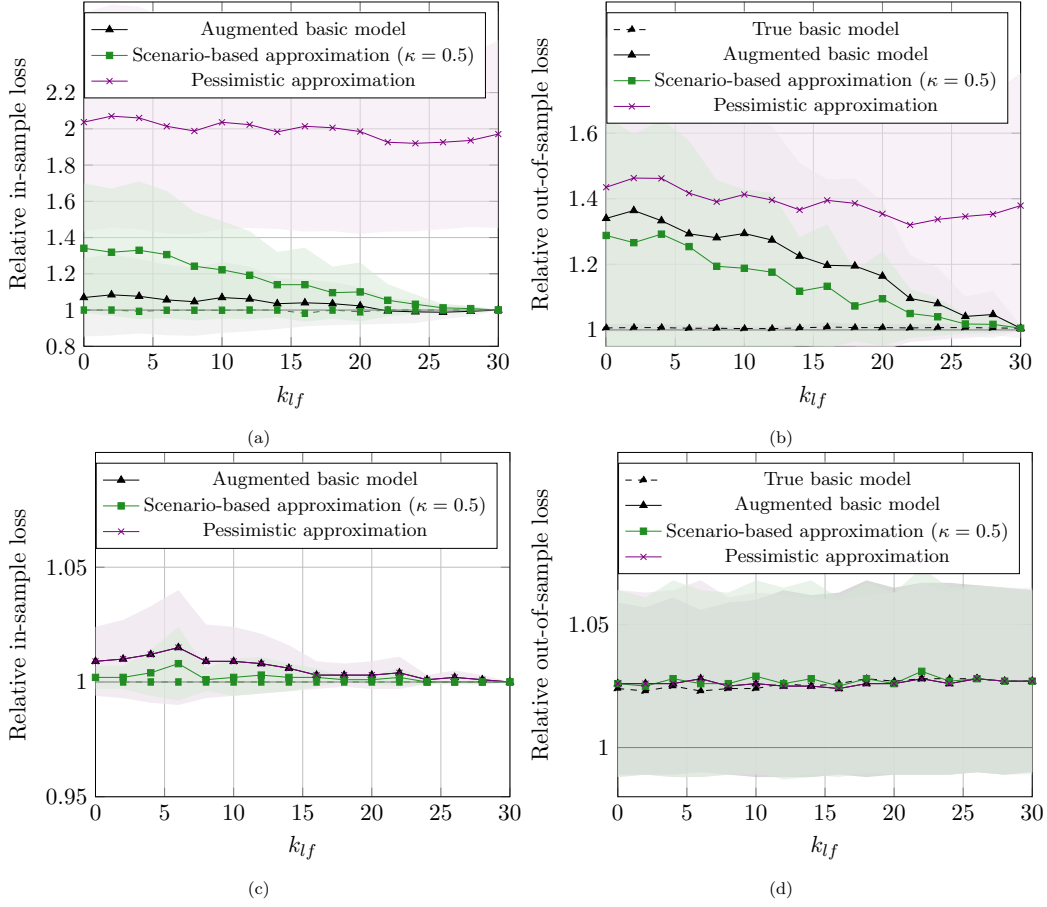


Figure 5: The average relative in-sample (6.9) (a, c) and out-of-sample (6.10) (b, d) loss of the *risk-neutral* leader (with MADs) as a function of the common sample size, k_{lf} , for $k_l = k_f = 30$ and $\delta_l = \delta_f = 0.1$, evaluated over 100 random test instances. The follower is assumed to be risk-averse (a, b) and risk-neutral (c, d). The dashed line corresponds to the empirical 5% percentile of the relative in-sample loss for the scenario-based semi-pessimistic approximation.

In our last experiment, we provide a similar comparison of three models, **[DRI-SP']**, **[DRI-P]** and **[DRI]**, but with a risk-neutral leader, i.e., $\alpha_l = 0$. The follower is assumed to be either risk-averse (Figures 5a and 5b) or risk-neutral (Figures 5c and 5d). In order address the unimodularity Assumption **A6'**, we simply replace the follower's feasible set $Y(\mathbf{x})$ with

$$Y_{uni}(\mathbf{x}) = \left\{ \mathbf{y} \in \mathbb{R}_+^n : \sum_{i=1}^n y_i \leq \lfloor 0.2n \rfloor, \mathbf{y} \leq \mathbf{U}(\mathbf{1} - \mathbf{x}) \right\}. \quad (6.11)$$

For the risk-averse follower, our observations are similar to those in the ambiguity-free case. However, with the risk-neutral follower, **[DRI-P]** and **[DRI]** demonstrate solid in-sample and out-of-sample performance, with a relatively small (1%) out-of-sample error. Indeed, when both decision-makers are risk-neutral and $\delta_l = \delta_f = 0.1$, one might expect that they operate in the sample average regime, aligning their objective functions; see Figure 2a. Therefore, by design, **[DRI-P]** and **[DRI]** provide identical optimal solutions and can be generally recommended for this particular case.

6.4. Analysis of running times

To maintain brevity, the detailed results of this section are relegated to Supplementary Material B, while a concise summary is presented below. Overall, the scenario-based approximation **[DRI-SP']** can be solved reasonably fast for small and medium-sized problem instances (with up to 30 binary decision variables for our test instances). The pessimistic approximation **[DRI-P]** is generally more computationally challenging and can only be solved with a relatively small sample size for the ambiguity-free leader, or with a small number of binary decision variables for the risk-neutral leader (approximately $k_l = 75$ and $n = 17$ in our test instances). Although our main focus is on the qualitative results, we believe that Algorithms 1 and 2 could be further enhanced to handle larger problem instances.

6.5. Summary of numerical results

Our computational results can be summarized as follows:

- Similar to the one-stage DRO models, calibrating the Wasserstein radius is essential for optimizing the model's out-of-sample performance. That is, the optimal Wasserstein radii in **[DRI]** significantly depend on the sample sizes of the leader and the follower, as well as the decision-makers' risk preferences. Our further analysis reveals that risk-aversion is essential for mitigating extremely small or large profits, while risk-neutral policies may offer a more effective approach for optimizing average gains.
- As shown in Figures 4b and 5b, the leader's incomplete knowledge of the follower's data may have a much greater impact than the distributional estimation errors. To address this issue, we suggest using either the scenario-based approximation **[DRI-SP']** or the pessimistic approximation **[DRI-P]**. Thus, **[DRI-SP']**, despite offering only asymptotic theoretical guarantees, exhibits strong in-sample and out-of-sample performance, even with a relatively small number of scenarios and significant uncertainty in the follower's data. In contrast, **[DRI-P]** tends to yield poor out-of-sample performance, unless the leader's and the follower's objective functions are well aligned.
- As a remark, **[DRI-SP']** may also be applied to the case where the follower's global parameters, α_f and ε_f , are subject to interval uncertainty. However, combining both data and parameter uncertainty is likely to make the scenario-based approximation more conservative, thereby aligning it more closely with the pessimistic approximation.

7. Conclusion

In this study, we explore a class of general linear interdiction problems with uncertainty in the follower's profit/cost vector. The profit vector is assumed to follow an unknown true distribution, while both the leader and the follower in our model can only estimate this distribution, based on their own historical data. Importantly, due to the conflicting objective criteria, the follower may choose to withhold some private historical data from the leader. To the best of our knowledge, this is the first data-driven interdiction model in the literature, where the decision-makers have asymmetric information regarding the data.

To address the distributional uncertainty, both decision-makers are assumed to solve conventional one-stage Wasserstein distributionally robust optimization (DRO) problems based on the conditional value-at-risk (CVaR). Moreover, we consider three distinct optimization models, reflecting different levels of the leader’s knowledge about the follower’s data. In the *basic model*, the leader has full knowledge of the follower’s data, and, therefore, the follower’s data set is contained in the leader’s. In contrast, under the *pessimistic* and the *semi-pessimistic* approximations, the leader either assumes the worst-case feasible follower’s policy or constructs an interval-based uncertainty set for the follower’s data.

We establish that the basic model is NP -hard, whereas both the pessimistic and the semi-pessimistic approximations are Σ_2^P -hard. Then, the basic and the semi-pessimistic models are addressed by leveraging a single-level mixed-integer linear programming (MILP) reformulation and discretization with a subsequent reformulation, respectively. In contrast, the pessimistic approximation is solved via a specialized Benders decomposition algorithm. Notably, we prove that, under a mild assumption, the basic model is asymptotically consistent, i.e., as the decision-makers acquire more data, their optimal solutions and the respective optimal objective function values converge to those of the underlying stochastic programming problem. Furthermore, we show that our discretization of the leader’s uncertainty set in the semi-pessimistic approximation is asymptotically robust. Put differently, as the number of scenarios increases, the resulting problem provides a robust approximation of the basic model with the true follower’s data set. To the best of our knowledge, these results have not been previously introduced in the bilevel optimization context and may provide a basis for addressing more complex hierarchical optimization problems under uncertainty.

Finally, we conduct a numerical study of all our models using a set of randomly generated instances of the packing interdiction problem. It turns out that the leader’s misspecification of the true follower’s policy in our bilevel context may have a greater impact than the individual errors of the decision-makers, which arise from their incomplete knowledge of the true distribution. Overall, our numerical results support the use of the scenario-based semi-pessimistic approximation, even when the follower’s data is subject to significant noise, and the pessimistic approximation when the leader’s and the follower’s objective functions are well aligned.

Competing Interests: None.

Availability of Data and Materials: Data were generated through numerical experiments, with the code available at: <https://github.com/sk19941995/Data-driven-interdiction>.

References

- [1] Atamtürk, A., Deck, C., and Jeon, H. (2020). Successive quadratic upper-bounding for discrete mean-risk minimization and network interdiction. *INFORMS Journal on Computing*, 32(2):346–355.
- [2] Azizi, E. and Seifi, A. (2024). Shortest path network interdiction with incomplete information: a robust optimization approach. *Annals of Operations Research*, 335(2):727–759.
- [3] Bartle, R. G. (2014). *The elements of integration and Lebesgue measure*. John Wiley & Sons.
- [4] Beck, Y., Ljubić, I., and Schmidt, M. (2023a). Exact methods for discrete γ -robust interdiction

- problems with an application to the bilevel knapsack problem. *Mathematical Programming Computation*, 15(4):733–782.
- [5] Beck, Y., Ljubić, I., and Schmidt, M. (2023b). A survey on bilevel optimization under uncertainty. *European Journal of Operational Research*, 311(2):401–426.
 - [6] Ben-Tal, A., El Ghaoui, L., and Nemirovski, A. (2009). *Robust optimization*, volume 28. Princeton University Press.
 - [7] Ben-Tal, A. and Nemirovski, A. (2002). Robust optimization—methodology and applications. *Mathematical Programming*, 92(3):453–480.
 - [8] Bertsimas, D., Gupta, V., and Kallus, N. (2018). Data-driven robust optimization. *Mathematical Programming*, 167:235–292.
 - [9] Bertsimas, D. and Sim, M. (2003). Robust discrete optimization and network flows. *Mathematical Programming*, 98(1-3):49–71.
 - [10] Birge, J. R. and Louveaux, F. (2011). *Introduction to stochastic programming*. Springer Science & Business Media, New York.
 - [11] Blanchet, J., Chen, L., and Zhou, X. Y. (2022). Distributionally robust mean-variance portfolio selection with Wasserstein distances. *Management Science*, 68(9):6382–6410.
 - [12] Bomze, I., Horländer, A., and Schmidt, M. (2025). Mixed-integer bilevel optimization with nonconvex quadratic lower-level problems: Complexity and a solution method. [url: https://optimization-online.org/wp-content/uploads/2024/12/indefinite-lower-level-qps.pdf](https://optimization-online.org/wp-content/uploads/2024/12/indefinite-lower-level-qps.pdf).
 - [13] Borrero, J. S., Prokopyev, O. A., and Sauré, D. (2016). Sequential shortest path interdiction with incomplete information. *Decision Analysis*, 13(1):68–98.
 - [14] Borrero, J. S., Prokopyev, O. A., and Sauré, D. (2019). Sequential interdiction with incomplete information and learning. *Operations Research*, 67(1):72–89.
 - [15] Buchheim, C., Henke, D., and Hommelsheim, F. (2021). On the complexity of robust bilevel optimization with uncertain follower’s objective. *Operations Research Letters*, 49(5):703–707.
 - [16] Calafiore, G. and Campi, M. C. (2005). Uncertain convex programs: randomized solutions and confidence levels. *Mathematical Programming*, 102:25–46.
 - [17] Calafiore, G. C. and Campi, M. C. (2006). The scenario approach to robust control design. *IEEE Transactions on Automatic Control*, 51(5):742–753.
 - [18] Chauhan, D., Unnikrishnan, A., Boyles, S. D., and Patil, P. N. (2024). Robust maximum flow network interdiction considering uncertainties in arc capacity and resource consumption. *Annals of Operations Research*, 335(2):689–725.
 - [19] Chen, Z., Kuhn, D., and Wiesemann, W. (2024). Data-driven chance constrained programs over Wasserstein balls. *Operations Research*, 72(1):410–424.
 - [20] Colson, B., Marcotte, P., and Savard, G. (2007). An overview of bilevel optimization. *Annals of Operations Research*, 153:235–256.
 - [21] Cormican, K. J., Morton, D. P., and Wood, R. K. (1998). Stochastic network interdiction. *Operations Research*, 46(2):184–197.

- [22] Delage, E. and Ye, Y. (2010). Distributionally robust optimization under moment uncertainty with application to data-driven problems. *Operations Research*, 58(3):595–612.
- [23] Dempe, S. (2002). *Foundations of bilevel programming*. Springer Science & Business Media, New York.
- [24] Dinitz, M. and Gupta, A. (2013). Packing interdiction and partial covering problems. In *International Conference on Integer Programming and Combinatorial Optimization*, pages 157–168. Springer.
- [25] Esfahani, P. M. and Kuhn, D. (2018). Data-driven distributionally robust optimization using the Wasserstein metric: Performance guarantees and tractable reformulations. *Mathematical Programming*, 171(1-2):115–166.
- [26] Gao, R. and Kleywegt, A. (2023). Distributionally robust stochastic optimization with Wasserstein distance. *Mathematics of Operations Research*, 48(2):603–655.
- [27] Grüne, C. and Wulf, L. (2025). Completeness in the polynomial hierarchy for many natural problems in bilevel and robust optimization. In *International Conference on Integer Programming and Combinatorial Optimization*, pages 256–269. Springer.
- [28] Hansen, P., Jaumard, B., and Savard, G. (1992). New branch-and-bound rules for linear bilevel programming. *SIAM Journal on Scientific and Statistical Computing*, 13(5):1194–1217.
- [29] Israeli, E. and Wood, R. K. (2002). Shortest-path network interdiction. *Networks*, 40(2):97–111.
- [30] Janjarassuk, U. and Linderoth, J. (2008). Reformulation and sampling to solve a stochastic network interdiction problem. *Networks*, 52(3):120–132.
- [31] Jeroslow, R. G. (1985). The polynomial hierarchy and a simple model for competitive analysis. *Mathematical Programming*, 32(2):146–164.
- [32] Kang, S. and Bansal, M. (2025). Distributionally risk-receptive and robust multistage stochastic integer programs and interdiction models. *Mathematical Programming*, pages 1–44.
- [33] Kantorovich, L. V. and Rubinshtein, S. (1958). On a space of totally additive functions. *Vestnik of the St. Petersburg University: Mathematics*, 13(7):52–59.
- [34] Ketkov, S. S. (2024). A study of distributionally robust mixed-integer programming with Wasserstein metric: on the value of incomplete data. *European Journal of Operational Research*, 313(2):602–615.
- [35] Kleinert, T., Labbé, M., Ljubić, I., and Schmidt, M. (2021). A survey on mixed-integer programming techniques in bilevel optimization. *EURO Journal on Computational Optimization*, 9:100007.
- [36] Kuhn, D., Esfahani, P. M., Nguyen, V. A., and Shafieezadeh-Abadeh, S. (2019). Wasserstein distributionally robust optimization: Theory and applications in machine learning. In *Operations Research & Management Science in the Age of Analytics*, pages 130–166. INFORMS TutORials in Operations Research.
- [37] Lei, X., Shen, S., and Song, Y. (2018). Stochastic maximum flow interdiction problems under heterogeneous risk preferences. *Computers & Operations Research*, 90:97–109.
- [38] Lim, C. and Smith, J. C. (2007). Algorithms for discrete and continuous multicommodity flow network interdiction problems. *IIE Transactions*, 39(1):15–26.

- [39] Nguyen, D. H. and Smith, J. C. (2022). Network interdiction with asymmetric cost uncertainty. *European Journal of Operational Research*, 297(1):239–251.
- [40] Pay, B. S., Merrick, J. R., and Song, Y. (2019). Stochastic network interdiction with incomplete preference. *Networks*, 73(1):3–22.
- [41] Rahimian, H. and Mehrotra, S. (2022). Frameworks and results in distributionally robust optimization. *Open Journal of Mathematical Optimization*, 3:1–85.
- [42] Rockafellar, R. T. and Uryasev, S. (2000). Optimization of conditional value-at-risk. *Journal of Risk*, 2:21–42.
- [43] Sadana, U. and Delage, E. (2023). The value of randomized strategies in distributionally robust risk-averse network interdiction problems. *INFORMS Journal on Computing*, 35(1):216–232.
- [44] Salmeron, J., Wood, K., and Baldick, R. (2004). Analysis of electric grid security under terrorist threat. *IEEE Transactions on Power Systems*, 19(2):905–912.
- [45] Shapiro, A., Dentcheva, D., and Ruszczyński, A. (2021). *Lectures on stochastic programming: modeling and theory*. SIAM.
- [46] Smith, J. C. and Lim, C. (2008). Algorithms for network interdiction and fortification games. In Chinchuluun, A., Pardalos, P. M., Migdalas, A., and Pitsoulis, L., editors, *Pareto optimality, game theory and equilibria*, pages 609–644. Springer.
- [47] Smith, J. C., Prince, M., and Geunes, J. (2013). Modern network interdiction problems and algorithms. In Pardalos, P. M., Du, D.-Z., and Graham, R. L., editors, *Handbook of Combinatorial Optimization*, pages 1949–1987. Springer.
- [48] Smith, J. C. and Song, Y. (2020). A survey of network interdiction models and algorithms. *European Journal of Operational Research*, 283(3):797–811.
- [49] Song, Y. and Shen, S. (2016). Risk-averse shortest path interdiction. *INFORMS Journal on Computing*, 28(3):527–539.
- [50] Wang, Z., You, K., Song, S., and Zhang, Y. (2020). Wasserstein distributionally robust shortest path problem. *European Journal of Operational Research*, 284(1):31–43.
- [51] Wiesemann, W., Kuhn, D., and Sim, M. (2014). Distributionally robust convex optimization. *Operations Research*, 62(6):1358–1376.
- [52] Zare, M. H., Borrero, J. S., Zeng, B., and Prokopyev, O. A. (2019). A note on linearized reformulations for a class of bilevel linear integer problems. *Annals of Operations Research*, 272:99–117.
- [53] Zeng, B. and An, Y. (2014). Solving bilevel mixed integer program by reformulations and decomposition. *Optimization Online*, pages 1–34.
- [54] Zenklusen, R. (2010). Matching interdiction. *Discrete Applied Mathematics*, 158(15):1676–1690.

Supplementary Material

for the manuscript

*Data-driven interdiction with asymmetric cost uncertainty:
a distributionally robust optimization approach*

Sergey S. Ketkov and Oleg A. Prokopyev

Department of Business Administration, University of Zurich

August 11, 2025

This file contains supplementary material including additional proofs, algorithmic descriptions, and computational results referenced in the main manuscript.

A. Supplementary proofs (Sections 3-5)

Proof of Lemma 1. First, following Example 3 in [2], we employ the minimax theorem to interchange the second and the third level problems in (3.3). That is, for any fixed $\mathbf{y} \in Y(\mathbf{x})$ we have:

$$\begin{aligned} \min_{\mathbb{Q}_f \in \mathcal{Q}_f} \rho_f(\mathbf{y}, \mathbb{Q}_f) &= \min_{\mathbb{Q}_f \in \mathcal{Q}_f} \max_{t_f \in \mathbb{R}} \left\{ t_f + \frac{1}{1 - \alpha_f} \mathbb{E}_{\mathbb{Q}_f} \{ (\mathbf{c}^\top \mathbf{y} - t_f)^- \} \right\} = \\ &= \max_{t_f \in \mathbb{R}} \left\{ t_f + \frac{1}{1 - \alpha_f} \min_{\mathbb{Q}_f \in \mathcal{Q}_f} \mathbb{E}_{\mathbb{Q}_f} \{ (\mathbf{c}^\top \mathbf{y} - t_f)^- \} \right\}. \end{aligned}$$

Hence, using Corollary 5.1 in [3], the worst-case expectation problem

$$\min_{\mathbb{Q}_f \in \mathcal{Q}_f} \mathbb{E}_{\mathbb{Q}_f} \{ (\mathbf{c}^\top \mathbf{y} - t_f)^- \}$$

can be equivalently reformulated as:

$$\max_{\boldsymbol{\nu}_f, \mathbf{s}_f, \lambda_f} \left\{ -\varepsilon_f \lambda_f - \frac{1}{k_f} \sum_{k \in K_f} s_f^{(k)} \right\} \quad (\text{S.1a})$$

$$\left. \begin{aligned} \text{s.t. } & -\hat{\mathbf{c}}_f^{(k)\top} \mathbf{y} + t_f + \boldsymbol{\Delta}_f^{(k)\top} \boldsymbol{\nu}_f^{(k)} \leq s_f^{(k)} \\ & \|\mathbf{B}^\top \boldsymbol{\nu}_f^{(k)} + \mathbf{y}\|_q \leq \lambda_f \\ & \boldsymbol{\nu}_f^{(k)} \geq \mathbf{0}, s_f^{(k)} \geq 0 \end{aligned} \right\} \forall k \in K_f \quad (\text{S.1b})$$

Formulation (3.4) is then obtained by combining (S.1) with the maximization with respect to t_f and \mathbf{y} .

Next, we consider the case where $p = 1$ and $q = \infty$; the opposite case is analogous and, therefore, is omitted for brevity. We note that, for each $k \in K_f$, constraints $\|\mathbf{B}^\top \boldsymbol{\nu}_f^{(k)} + \mathbf{y}\|_\infty \leq \lambda_f$ can be equivalently expressed as:

$$-\lambda_f \mathbf{1} \leq \mathbf{B}^\top \boldsymbol{\nu}_f^{(k)} + \mathbf{y} \leq \lambda_f \mathbf{1}. \quad (\text{S.2})$$

Let $\bar{\boldsymbol{\mu}}_f^{(k)} \in \mathbb{R}_+^n$ and $\underline{\boldsymbol{\mu}}_f^{(k)} \in \mathbb{R}_+^n$, $k \in K_f$, be dual variables corresponding to the first and the second inequality constraints in (S.2). Also, given that $d_f = \dim(\mathbf{f})$, let $\boldsymbol{\beta}_f \in \mathbb{R}_+^{d_f}$ and $\boldsymbol{\gamma}_f \in \mathbb{R}_+^{k_f}$, be dual variables corresponding to constraints (3.4b) and the first set of constraints in (3.4c), respectively. Then, the dual reformulation of (3.4) can be obtained by using the standard LP duality, and the result follows. \square

Proof of Theorem 1. First, assume that the follower's decision, \mathbf{y} , in [DRI] is fixed. Then, analogously to the proof of Lemma 1, the leader's problem

$$\min_{\mathbf{x} \in X} \max_{\mathbf{Q}_l \in \mathcal{Q}_l} \min_{t_l \in \mathbb{R}} \left\{ t_l + \frac{1}{1 - \alpha_l} \mathbb{E}_{\mathbf{Q}_l} \{ (\mathbf{c}^\top \mathbf{y} - t_l)^+ \} \right\}$$

can be expressed as:

$$\min_{\mathbf{x}, \boldsymbol{\nu}_l, s_l, \lambda_l, t_l} \left\{ t_l + \frac{1}{1 - \alpha_l} (\varepsilon_l \lambda_l + \frac{1}{k_l} \sum_{k \in K_l} s_l^{(k)}) \right\} \quad (\text{S.3a})$$

$$\text{s.t. } \mathbf{x} \in X \quad (\text{S.3b})$$

$$\left. \begin{aligned} \hat{\mathbf{c}}_l^{(k)\top} \mathbf{y} - t_l + \boldsymbol{\Delta}_l^{(k)\top} \boldsymbol{\nu}_l^{(k)} &\leq s_l^{(k)} \\ \|\mathbf{B}^\top \boldsymbol{\nu}_l^{(k)} - \mathbf{y}\|_q &\leq \lambda_l \\ \boldsymbol{\nu}_l^{(k)} &\geq \mathbf{0}, s_l^{(k)} \geq 0. \end{aligned} \right\} \forall k \in K_l \quad (\text{S.3c})$$

Next, we need to ensure that \mathbf{y} is an optimal solution of the follower's problem (3.3) and incorporate the minimization with respect to \mathbf{y} into (S.3). We enforce primal and dual feasibility by leveraging constraints (3.4b)–(3.4d) and (3.5b)–(3.5f), respectively. These constraints, along with the strong duality condition (3.6e), guarantee optimality of \mathbf{y} and result in a single-level reformulation (3.6). \square

Proof of Lemma 3. By Lemma 1, $v_f(\mathbf{y}, \hat{\mathbf{C}}_f)$ coincides with the optimal objective function value of (3.4) for a fixed $\mathbf{y} \in \bar{Y}(\mathbf{x})$. Alternatively, by using linear programming duality, we have:

$$v_f(\mathbf{y}, \hat{\mathbf{C}}_f) = \min_{\bar{\boldsymbol{\mu}}_f, \underline{\boldsymbol{\mu}}_f, \boldsymbol{\gamma}_f} \left\{ \sum_{k \in K_f} -(\bar{\boldsymbol{\mu}}_f^{(k)} - \underline{\boldsymbol{\mu}}_f^{(k)})^\top \mathbf{y} + \sum_{k \in K_f} (\boldsymbol{\gamma}_f^{(k)} \hat{\mathbf{c}}_f^{(k)})^\top \mathbf{y} \right\} \quad (\text{S.4a})$$

$$\left. \begin{aligned} \text{s.t. } \boldsymbol{\gamma}_f^{(k)} \boldsymbol{\Delta}_f^{(k)} + \mathbf{B}(\bar{\boldsymbol{\mu}}_f^{(k)} - \underline{\boldsymbol{\mu}}_f^{(k)}) &\geq \mathbf{0} \\ 0 \leq \boldsymbol{\gamma}_f^{(k)} &\leq \frac{1}{(1 - \alpha_f)k_f} \\ \bar{\boldsymbol{\mu}}_f^{(k)} &\geq \mathbf{0}, \underline{\boldsymbol{\mu}}_f^{(k)} \geq \mathbf{0} \end{aligned} \right\} \forall k \in K_f \quad (\text{S.4b})$$

$$\left\| \sum_{k \in K_f} (\bar{\boldsymbol{\mu}}_f^{(k)} + \underline{\boldsymbol{\mu}}_f^{(k)}) \right\|_p \leq \frac{1}{1 - \alpha_f} \varepsilon_f \quad (\text{S.4c})$$

$$\sum_{k \in K_f} \gamma_f^{(k)} = 1. \quad (\text{S.4d})$$

It is rather straightforward to verify that the dual objective function in (S.4) is continuous, and the corresponding feasible set is non-empty and compact. Furthermore, for any $\mathbf{y} \in \bar{Y}(\mathbf{x})$, the primal problem (3.4) is feasible. Hence, strong duality holds and $v_f(\mathbf{y}, \hat{\mathbf{C}}_f)$ is continuous by Berge's maximum theorem [1]. Finally, given continuity of $v_f(\mathbf{y}, \hat{\mathbf{C}}_f)$ and Assumption **A1**, the same reasoning shows that $\hat{V}_f(\mathbf{x}, \hat{\mathbf{C}}_f)$ defined by equation (3.11) is non-empty and upper semicontinuous. \square

Proof of Theorem 4. First, following the proof of Theorem 1, the second-level problem

$$\max_{\mathbf{y} \in Y(\mathbf{x})} \max_{\mathbb{Q}_l \in \mathcal{Q}_l} \min_{t_l \in \mathbb{R}} \left\{ t_l + \frac{1}{1 - \alpha_l} \mathbb{E}_{\mathbb{Q}_l} \{ (\mathbf{c}^\top \mathbf{y} - t_l)^+ \} \right\}$$

can be expressed as the following max-min problem:

$$\max_{\mathbf{y} \in Y(\mathbf{x})} \min_{\boldsymbol{\nu}_l, \mathbf{s}_l, \lambda_l, t_l} \left\{ t_l + \frac{1}{1 - \alpha_l} (\varepsilon_l \lambda_l + \frac{1}{k_l} \sum_{k \in K_l} s_l^{(k)}) \right\} \quad (\text{S.5a})$$

$$\left. \begin{aligned} \text{s.t. } & \hat{\mathbf{c}}_l^{(k)\top} \mathbf{y} - t_l + \boldsymbol{\Delta}_l^{(k)\top} \boldsymbol{\nu}_l^{(k)} \leq s_l^{(k)} \\ & \|\mathbf{B}^\top \boldsymbol{\nu}_l^{(k)} - \mathbf{y}\|_q \leq \lambda_l \\ & \boldsymbol{\nu}_l^{(k)} \geq \mathbf{0}, s_l^{(k)} \geq 0 \end{aligned} \right\} \forall k \in K_l. \quad (\text{S.5b})$$

Then, we only need to derive an equivalent dual reformulation of the second-level optimization problem in (S.5). If we denote by $\tilde{\gamma}_l \in \mathbb{R}_+^{k_l}$ and $(\underline{\boldsymbol{\mu}}_l^{(k)}, \bar{\boldsymbol{\mu}}_l^{(k)}) \in \mathbb{R}_+^n \times \mathbb{R}_+^n$, respectively, the dual variables corresponding to the first and the second set of constraints in (S.5b), then (S.5) can be equivalently reformulated as:

$$\begin{aligned} & \max_{\mathbf{y}, \underline{\boldsymbol{\mu}}_l, \bar{\boldsymbol{\mu}}_l, \tilde{\gamma}_l} \left\{ \sum_{k \in K_l} (\tilde{\gamma}_l^{(k)} \hat{\mathbf{c}}_l^{(k)} - \bar{\boldsymbol{\mu}}_l^{(k)} + \underline{\boldsymbol{\mu}}_l^{(k)})^\top \mathbf{y} \right\} \\ \text{s.t. } & \mathbf{y} \in Y(\mathbf{x}) \\ & \left. \begin{aligned} & \tilde{\gamma}_l^{(k)} \boldsymbol{\Delta}_l^{(k)} + \mathbf{B}(\bar{\boldsymbol{\mu}}_l^{(k)} - \underline{\boldsymbol{\mu}}_l^{(k)}) \geq \mathbf{0} \\ & 0 \leq \tilde{\gamma}_l^{(k)} \leq \frac{1}{(1 - \alpha_l) k_l} \\ & \bar{\boldsymbol{\mu}}_l^{(k)}, \underline{\boldsymbol{\mu}}_l^{(k)} \geq \mathbf{0} \end{aligned} \right\} \forall k \in K_l \\ & \left\| \sum_{k \in K_l} (\bar{\boldsymbol{\mu}}_l^{(k)} + \underline{\boldsymbol{\mu}}_l^{(k)}) \right\|_p \leq \frac{1}{1 - \alpha_f} \varepsilon_l \\ & \sum_{k \in K_l} \tilde{\gamma}_l^{(k)} = 1, \end{aligned}$$

where $\boldsymbol{\Delta}_l^{(k)} = \mathbf{b} - \mathbf{B}\hat{\mathbf{c}}_l^{(k)} \geq \mathbf{0}$ for each $k \in K_l$. Finally, reformulation (4.8) is obtained by introducing new variables $\boldsymbol{\xi}_l^{(k)} = k_l(1 - \alpha_l)(\bar{\boldsymbol{\mu}}_l^{(k)} - \underline{\boldsymbol{\mu}}_l^{(k)})$, $\boldsymbol{\eta}_l^{(k)} = k_l(1 - \alpha_l)(\bar{\boldsymbol{\mu}}_l^{(k)} + \underline{\boldsymbol{\mu}}_l^{(k)})$ and $\gamma_l^{(k)} = k_l(1 - \alpha_l)\tilde{\gamma}_l^{(k)}$ for each $k \in K_l$. \square

Proof of Theorem 6. First, for each scenario $r \in R_l$, we introduce a new variable

$$\begin{aligned} z^{(r)} &:= \min_{\mathbf{y}^{(r)}} \left\{ \max_{\mathbb{Q}_l^{(r)} \in \mathcal{Q}_l} \rho_l(\mathbf{y}^{(r)}, \mathbb{Q}_l^{(r)}) \right\} \\ \text{s.t. } \mathbf{y}^{(r)} &\in \operatorname{argmax}_{\tilde{\mathbf{y}}^{(r)} \in Y(\mathbf{x})} \left\{ \min_{\mathbb{Q}_f^{(r)} \in \mathcal{Q}_f} \rho_f(\tilde{\mathbf{y}}^{(r)}, \mathbb{Q}_f^{(r)}) \right\}, \end{aligned}$$

where $\mathcal{Q}_f^{(r)} := \mathcal{Q}_f(\hat{\mathbf{C}}_f^{(r)})$. Then, **[DRI-SP']** can be expressed as:

$$\min_{\mathbf{x} \in X} \max_{r \in R_l} z^{(r)} = \min_{\mathbf{x}, z} z \quad (\text{S.6a})$$

$$\text{s.t. } \mathbf{x} \in X \quad (\text{S.6b})$$

$$z \geq z^{(r)} \quad \forall r \in R_l. \quad (\text{S.6c})$$

Furthermore, by the definition of $z^{(r)}$, constraints (S.6c) for each $r \in R_l$ can be reduced to the following system of inequalities:

$$\begin{cases} z \geq \max_{\mathbb{Q}_l^{(r)} \in \mathcal{Q}_l} \rho_l(\mathbf{y}^{(r)}, \mathbb{Q}_l^{(r)}) \\ \mathbf{y}^{(r)} \in \operatorname{argmax}_{\tilde{\mathbf{y}}^{(r)} \in Y(\mathbf{x})} \left\{ \min_{\mathbb{Q}_f^{(r)} \in \mathcal{Q}_f} \rho_f(\tilde{\mathbf{y}}^{(r)}, \mathbb{Q}_f^{(r)}) \right\}. \end{cases}$$

The final reformulation (5.7) is then obtained by leveraging Theorem 1. \square

B. Implementation details and auxiliary computational results (Section 6)

Benders decomposition algorithm for the risk-neutral problem (4.14). Under Assumption **A6'**, the risk-neutral pessimistic approximation (4.14) can be expressed as:

$$\min_{\mathbf{x}, z} z \quad (\text{S.1a})$$

$$\text{s.t. } \mathbf{x} \in X \quad (\text{S.1b})$$

$$z \geq \max_{(\boldsymbol{\xi}_l, \boldsymbol{\eta}_l) \in \Xi} \left\{ \bar{\mathbf{c}}_l^\top \mathbf{y} + \frac{1}{k_l} \sum_{k \in K_l} (-\boldsymbol{\xi}_l^{(k)\top} \mathbf{y}) \right\} - M \mathbf{x}^\top \mathbf{y} \quad \forall \mathbf{y} \in \bar{Y}, \quad (\text{S.1c})$$

where $\bar{\mathbf{c}}_l = \frac{1}{k_l} \sum_{k \in K_l} \mathbf{c}_l^{(k)}$, $M \in \mathbb{R}_+$ is a sufficiently large constant,

$$\Xi := \{(\boldsymbol{\xi}_l, \boldsymbol{\eta}_l) : \text{constraints (4.14c)–(4.14d) hold}\} \quad \text{and} \quad \bar{Y} = \{\mathbf{y} \in \mathbb{Z}_+^n : \tilde{\mathbf{F}}\mathbf{y} \leq \tilde{\mathbf{f}}, \mathbf{y} \leq \mathbf{U}\mathbf{1}\}.$$

In particular, since $Y(\mathbf{x})$ is non-empty (recall Assumption **A1**), by selecting a sufficiently large M , we implicitly enforce that optimal $\mathbf{y}^* \in \bar{Y}$ is such that $y_i^* = 0$ whenever $x_i^* = 1$, $i \in N := \{1, \dots, n\}$.

Next, by leveraging a dual reformulation of (S.1c) for a given subset $\hat{Y} \subseteq \bar{Y}$, we define a master problem:

$$[\mathbf{MP}'(\hat{Y})] : \min_{\mathbf{x}, \boldsymbol{\nu}, z} z \quad (\text{S.2a})$$

$$\text{s.t. } \mathbf{x} \in X \quad (\text{S.2b})$$

$$z \geq \varepsilon_l \lambda(\mathbf{y}) + \bar{\mathbf{c}}_l^\top \mathbf{y} - M \mathbf{x}^\top \mathbf{y} + \frac{1}{k_l} \sum_{k \in K_l} \Delta_l^{(k)\top} \boldsymbol{\nu}^{(k)}(\mathbf{y}) \quad \forall \mathbf{y} \in \hat{Y} \quad (\text{S.2c})$$

$$\left. \begin{aligned} \|\mathbf{B}^\top \boldsymbol{\nu}^{(k)}(\mathbf{y}) - \mathbf{y}\|_q &\leq \lambda(\mathbf{y}) \\ \boldsymbol{\nu}^{(k)}(\mathbf{y}) &\geq \mathbf{0} \end{aligned} \right\} \forall k \in K_l, \forall \mathbf{y} \in \hat{Y}, \quad (\text{S.2d})$$

with $\Delta_l^{(k)} = \mathbf{b} - \mathbf{B}\hat{\mathbf{c}}_l^{(k)}$, $k \in K_l$, and the second-level subproblem

$$[\text{Sub}'(\mathbf{x})] : \max_{\mathbf{y}, \boldsymbol{\xi}_l, \boldsymbol{\eta}_l} \left\{ \frac{1}{k_l} \sum_{k \in K_l} (\hat{\mathbf{c}}_l^{(k)} - \boldsymbol{\xi}_l^{(k)})^\top \mathbf{y} : \mathbf{y} \in Y(\mathbf{x}), (\boldsymbol{\xi}_l, \boldsymbol{\eta}_l) \in \Xi \right\}. \quad (\text{S.3})$$

Notably, Ξ is non-empty and compact by design, ensuring that $[\text{MP}'(\hat{Y})]$ admits a finite optimum.

Algorithm 2: A basic Benders decomposition-based algorithm for (4.14).

```

1 Input: the risk-neutral problem (4.14) and a tolerance level  $\delta \in \mathbb{R}_+$ .
2 Output: an optimal solution  $\hat{\mathbf{x}}_p^* \in X$  and the optimal objective function value  $\hat{z}_p^*$ .
3  $LB \leftarrow -\infty, UB \leftarrow \infty$ 
4  $\hat{\mathbf{x}}^* \leftarrow \mathbf{0}, \hat{Y} \leftarrow \emptyset$ 
5 while  $UB - LB > \delta$  do
6    $(\hat{\mathbf{y}}^*, \hat{\boldsymbol{\xi}}_l^*, \hat{\boldsymbol{\eta}}_l^*) \leftarrow$  an optimal solution of  $[\text{Sub}'(\hat{\mathbf{x}}^*)]$ 
7    $UB' \leftarrow$  the optimal objective function value of  $[\text{Sub}'(\hat{\mathbf{x}}^*)]$ 
8   if  $UB' < UB$  then
9      $(\hat{\mathbf{x}}_p^*, \hat{z}_p^*) \leftarrow (\hat{\mathbf{x}}^*, UB')$ 
10     $UB \leftarrow UB'$ 
11   end
12    $\hat{Y} \leftarrow \hat{Y} \cup \{\hat{\mathbf{y}}^*\}$ 
13    $(\hat{\mathbf{x}}^*, \hat{z}^*) \leftarrow$  an optimal solution of  $[\text{MP}'(\hat{Y})]$ ,
14    $LB \leftarrow \hat{z}^*$ 
15 end
16 return  $\hat{\mathbf{x}}_p^*, \hat{z}_p^*$ 

```

As a result, the risk-neutral pessimistic approximation (4.14) can be solved in the same way as the ambiguity-free problem (4.9); we refer to Algorithm 2 for the pseudocode. Similar to Algorithm 1, the correctness of Algorithm 2 is ensured by the finiteness of \bar{Y} .

Linearization of the MILP reformulation (3.6). By leveraging the structure of the packing interdiction problem (6.1), it can be observed that:

$$(-\mathbf{L}\mathbf{x} + \mathbf{f})^\top \boldsymbol{\beta}_f = \tilde{\mathbf{f}}^\top \boldsymbol{\beta}_f^{(1)} + \mathbf{U}(\mathbf{1} - \mathbf{x})^\top \boldsymbol{\beta}_f^{(2)},$$

where $\boldsymbol{\beta}_f^{(1)} \in \mathbb{R}_+^{\tilde{d}_f}$ and $\boldsymbol{\beta}_f^{(2)} \in \mathbb{R}_+^n$. Therefore, we only need to linearize the products of binary variables \mathbf{x}

and continuous variables $\beta_f^{(2)}$. Given that $p_i = (1 - x_i)(\beta_f^{(2)})_i$ for $i \in N$, we apply the standard McCormick linearization [4], i.e.,

$$\begin{cases} 0 \leq p_i \leq (\beta_f^{(2)})_i \\ p_i \leq M(1 - x_i) \\ p_i \geq (\beta_f^{(2)})_i - Mx_i, \end{cases}$$

where $M \in \mathbb{R}_+$ is a valid upper bound on $(\beta_f^{(2)})_i$, $i \in N$.

Finally, to select M , we note that:

$$\mathbf{U}(\mathbf{1} - \mathbf{x})^\top \beta_f^{(2)} = (\mathbf{1} - \mathbf{x})^\top \beta_f^{(2)} \leq n.$$

Here, we use the fact that $\mathbf{U} = \mathbf{I}$, $\tilde{\mathbf{f}} > 0$ and that the follower's optimal objective function value given by the left-hand side of (3.6e) is bounded from above by n ; recall (6.3). On the other hand, by leveraging (3.5b), we observe that:

$$\mathbf{F}^\top \beta_f = \tilde{\mathbf{F}}^\top \beta_f^{(1)} + \beta_f^{(2)} \geq \sum_{k \in K_f} \gamma_f^{(k)} \hat{\mathbf{c}}_f^{(k)} - \sum_{k \in K_f} (\bar{\boldsymbol{\mu}}_f^{(k)} - \underline{\boldsymbol{\mu}}_f^{(k)}).$$

Furthermore, for each $i \in N$, we have:

$$\left(\sum_{k \in K_f} \gamma_f^{(k)} \hat{\mathbf{c}}_f^{(k)} - \sum_{k \in K_f} (\bar{\boldsymbol{\mu}}_f^{(k)} - \underline{\boldsymbol{\mu}}_f^{(k)}) \right)_i \leq \left(\sum_{k \in K_f} \gamma_f^{(k)} + \sum_{k \in K_f} \underline{\boldsymbol{\mu}}_f^{(k)} \right)_i \leq 1 + \frac{\varepsilon_f}{1 - \alpha_f},$$

where the last inequality exploits (3.5d) and (3.5e) with $p = 1$.

As a result, if

$$(\beta_f^{(2)})_i > \max \left\{ n; 1 + \frac{\varepsilon_f}{1 - \alpha_f} \right\}$$

for some $i \in N$, then $x_i = 1$ and the constraint (3.5b) for $i \in N$ is non-binding. Therefore, we can set

$$(\beta_f^{(2)})_i = M := \max \left\{ n; 1 + \frac{\varepsilon_f}{1 - \alpha_f} \right\},$$

without affecting constraints (3.6e) and (3.5b).

The same upper bound for dual variables, M , is used in the scenario-based formulation (5.7). A similar reasoning implies that the dual variables $\beta_l(\gamma_l)$ for every $\gamma_l \in \Gamma$ in the ambiguity-free master problem (4.12) are bounded from above by $M = \max\{1; n\}$. In conclusion, we use $M = n$ in the risk-neutral master problem (S.2). Other products of variables arising in the subproblems (4.13) and (S.3) can be linearized by leveraging somewhat straightforward upper bounds on \mathbf{y} , $\boldsymbol{\gamma}_l$ and $\boldsymbol{\xi}_l$. \square

Analysis of running times. Here, we provide a brief analysis of running times for all three considered formulations. The leader's and the follower's data sets, $\hat{\mathbf{C}}_l$ and $\hat{\mathbf{C}}_f$, are assumed to be identical and, therefore, [DRI] is simply referred to as a basic model. First, in Figures S1a and S1b, we examine how solution times for [DRI] and [DRI-SP'] scale with the samples sizes, k_l and k_f ,

and the problem size n , respectively. All plots are presented on a log-log scale. For each parameter value, we report the average solution times (with MADs) over 10 randomly generated test instances of the packing interdiction problem (6.1). The time limit is set to 60 minutes. If at least one of the 10 test instances remains unsolved within this limit, we discard the corresponding parameter value, along with all larger values.

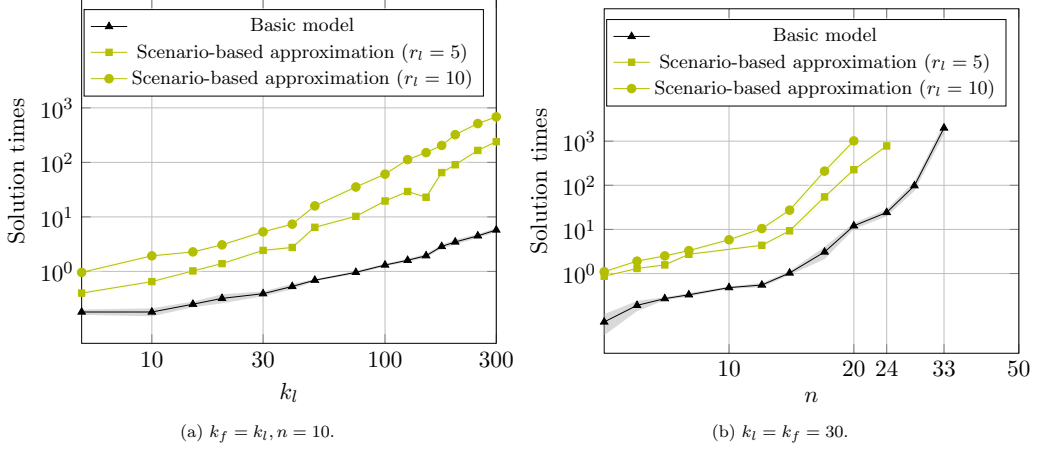


Figure S1: Average solution times in seconds (with MADs) of the basic and semi-pessimistic formulations as a function of $k_l = k_f$ (a) and n (b), for $\delta_l = \delta_f = 0.1$, $k_{lf} = \lfloor \frac{2}{3}k_f \rfloor$ and $\kappa = 0.2$, evaluated over 10 random test instances. The time limit is set to 60 minutes. If at least one out of the 10 test instances is not solved within this limit, we discard the corresponding value of parameter, along with all larger values.

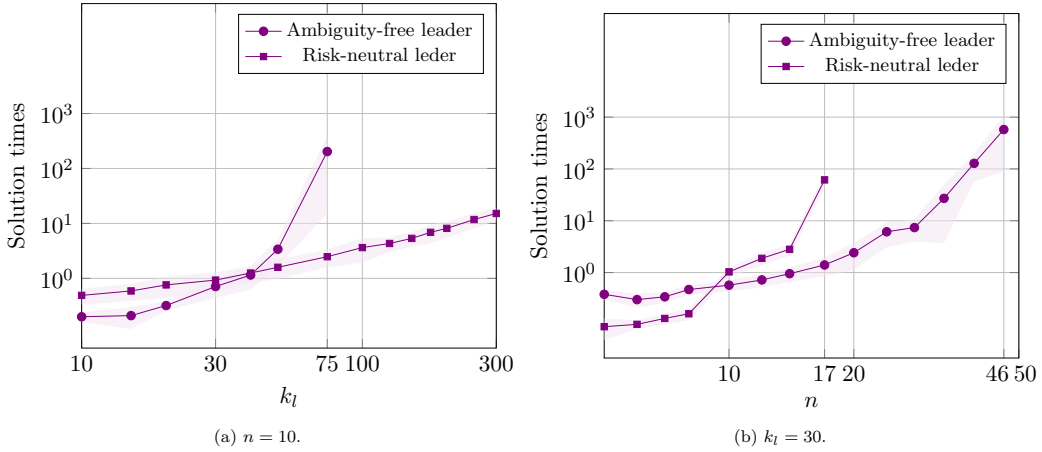


Figure S2: Average solution times in seconds (with MADs) of the pessimistic formulation as a function of k_l (a) and n (b), for $\delta_l = 0.1$ and $\alpha_l = 0.9$, evaluated over 10 random test instances. The time limit is set to 60 minutes. If at least one out of the 10 test instances is not solved within this limit, we discard the corresponding value of parameter, along with all larger values.

Figure S1 suggests that solution times scale well with k_l , k_f , and r_l , showing a growth pattern that is approximately polynomial. However, intuitively, when n increases, the number of binary variables in the MILP reformulations (3.6) and (5.7) also grows, leading to an exponential increase in the running time. In this regard, we recall that even the deterministic version of our problem, [DP], is *NP*-hard in the strong sense. As a result, we suggest using models [DRI] and [DRI-SP'] for moderately-sized problem instances, with up to around 30 leader's decision variables.

Then, we analyze how solution times for the pessimistic approximation **[DRI-P]** scale in k_l and n ; see Figures S2a and S2b, respectively. The parameter k_l is adjusted to satisfy Assumption **A6**. We observe that **[DRI-P]** for the ambiguity-free leader scales more efficiently with n , while the approximation for the risk-neutral leader scales better with k_l . This observation can be explained by the design of Algorithms 1 and 2. Thus, Algorithm 1 for the ambiguity-free leader enumerates solutions in the discrete set Γ given by equation (4.11), whose size grows exponentially with the increase of k_l . At the same time, Algorithm 2 operates with the discrete set \hat{Y} , whose size is exponential in n ; recall (6.11). \square

References

- [1] Berge, C. (1877). *Topological spaces: Including a treatment of multi-valued functions, vector spaces and convexity*. Oliver & Boyd.
- [2] Delage, E. and Ye, Y. (2010). Distributionally robust optimization under moment uncertainty with application to data-driven problems. *Operations Research*, 58(3):595–612.
- [3] Esfahani, P. M. and Kuhn, D. (2018). Data-driven distributionally robust optimization using the Wasserstein metric: Performance guarantees and tractable reformulations. *Mathematical Programming*, 171(1-2):115–166.
- [4] McCormick, G. P. (1976). Computability of global solutions to factorable nonconvex programs: Part I – convex underestimating problems. *Mathematical Programming*, 10(1):147–175.